iScience

Article

Mechanism analysis of microwave radiation generated by transverse magnetized plasma excited by electron beam

Graphical abstract

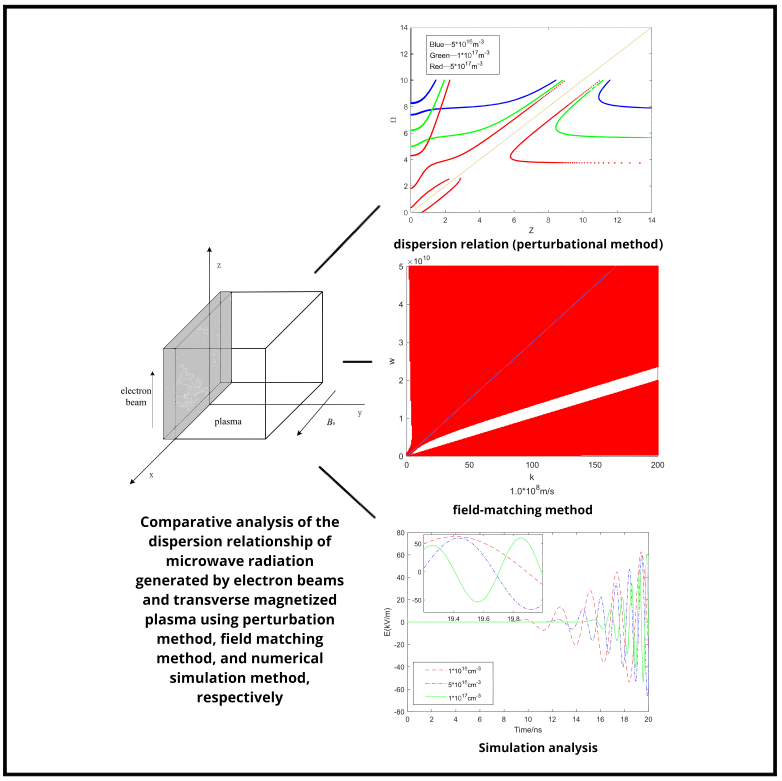

Highlights

- Derived the dispersion relationship of transverse magnetized plasma microwave
- Comparative analysis of dispersion curves derived by different methods
- Analysis of the influence of different parameters on dispersion curve

Authors

S. Gao, J.X. Liu, J.K. Zhang

Correspondence

gs59519829@126.com

In brief

Natural sciences; Physics; Electromagnetics

Gao et al., 2024, iScience *27*, 111031
December 20, 2024
https://doi.org/10.1016/j.isci.2024.111031

CellPress

iScience

CellPress
OPEN ACCESS

Article

Mechanism analysis of microwave radiation generated by transverse magnetized plasma excited by electron beam

S. Gao,[1,2,*] J.X. Liu,[1] and J.K. Zhang[1]
[1]School of Electrical and Information, ChangZhou Institute of Technology, ChangZhou 213032, China
[2]Lead contact
*Correspondence: gs59519829@126.com
https://doi.org/10.1016/j.isci.2024.111031

SUMMARY

This article establishes a physical model of the interaction between surface electron beams and plasma with a transverse magnetic field. The dispersion relationship between electron beam and transverse magnetized plasma interaction was derived using perturbation method and field matching method, respectively. We studied the effects of magnetic field, plasma density, electron beam density, and electron beam velocity on radiation frequency and bandwidth. The correctness of the aforementioned results was further verified through simulation analysis. The results show that the stronger the transverse magnetic field, the higher the radiation frequency, but the smaller the radiation bandwidth; the higher the plasma density, electron beam density, or electron beam velocity, the corresponding radiation frequency and radiation bandwidth increase accordingly.

INTRODUCTION

The problem of plasma broadband microwave radiation belongs to the field of high-power microwave (HPM) technology.[1–4] High-power microwave technology has developed with disciplines, such as pulse power technology, microwave electronics, relativistic electronics, high-current charged particle beam physics, plasma physics, and gas discharge physics. The development of high-power microwave comes from its applications in military, energy, and scientific research.

Through early experiments and theoretical analysis, the preliminary mechanism of broadband microwave radiation generated by the interaction between electron beams and plasma is as follows[5]: first, plasma is formed and then electron beams are emitted and incident into the plasma. The plasma is magnetized by a magnetic field excited by an electron beam, making it an uneven anisotropic medium. When electromagnetic waves propagate along the axial and radial directions of the plasma, they become slow waves; the subsequent electron beam passing through magnetized plasma will excite Cherenkov radiation.[6,7] Due to the inverse Landau damping, the free energy in the plasma will be converted into the energy of electromagnetic waves. The interaction between electron beams and plasma occurs, and the beam plasma interaction causes various instability.[8,9] These complex interactions between electron beams, waves, and plasma can radiate electromagnetic waves and enhance them.

When an electron beam interacts with a plasma, the transverse magnetic field not only magnetizes the plasma but also changes the trajectory of the electron beam, which is different from the trajectory of the electron beam passing through an unmagnetized plasma. This article derives the dispersion relationship of microwave radiation generated by the interaction between beam and transverse magnetized plasma using perturbation method and field matching method and analyzes the influence of different parameters on the dispersion curve.

Deduction of dispersion relationship-perturbation method

The physical model of plasma microwave radiation is shown in Figure 1. The surface electron beam is used to interact with plasma. The electron beam moves in the z-direction.

We are concerned with the transverse magnetic wave propagating perpendicular to the direction of the induced magnetic field, $\vec{k}\cdot B_x = 0$, B_x is the induced magnetic field in the radiated electromagnetic field. B_0 is the uniformly applied x-term magnetic field externally. In the experiment, permanent magnets can be used to achieve. Assume that the direction of B_x is the x direction, so the electromagnetic wave has two components: E_y and E_z, so it can be set:

$$E_{1y} = E_y e^{i\left(\vec{k}_y\cdot\vec{y}+\vec{k}_z\cdot\vec{z}-\omega t\right)} \quad \text{(Equation 1)}$$

$$E_{1z} = E_z e^{i\left(\vec{k}_y\cdot\vec{y}+\vec{k}_z\cdot\vec{z}-\omega t\right)} \quad \text{(Equation 2)}$$

$$B_1 = B_{1x}\vec{x}e^{i\left(\vec{k}_y\cdot\vec{y}+\vec{k}_z\cdot\vec{z}-\omega t\right)} \quad \text{(Equation 3)}$$

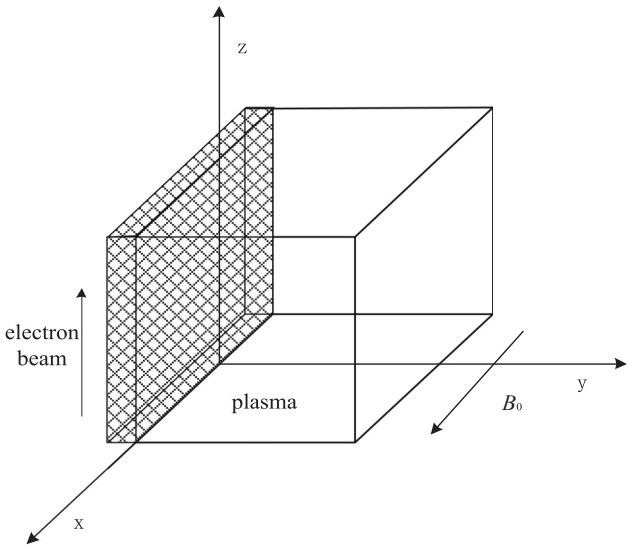

Figure 1. Physical model of plasma microwave radiation

A physical model of the interaction between a surface electron beam and a transverse magnetized plasma, with the magnetic field direction perpendicular to the direction of electron beam motion.

When discussing the weak interaction of the electron beam and plasma, it can be assumed that the ions are not moving, and the relevant physical quantities can be expressed as constants in the equilibrium state plus varying perturbations, that is $f = f_0 + f_1$. Subscript 0 represents the quantity in the equilibrium state, subscript 1 represents the disturbance quantity, disturbance quantity is $f_1 \propto \exp(ik_z z + ik_y y - i\omega t)$, and $f_0 \gg f_1$, k_z, k_y, and ω are wave numbers and angular frequencies respectively.

The aforementioned model can be seen as the interaction between two types of plasmas.[10–12] The electron beam can be regarded as a non-neutral plasma in high-speed motion, therefore it satisfies the equations of particle number conservation and momentum conservation. Due to the relativistic velocity of the electron beam, a relativistic factor is introduced in Equation 7. Similarly, the plasma itself also satisfies the equations of particle number conservation and momentum conservation. Compared with high-energy electron beams, the initial velocity of the plasma is 0, and the ion term equations (ion number momentum conservation and particle number conservation) in the plasma are ignored because ions mainly produce ion sound waves. Equations 8 and 9 are Maxwell's equations, while Equation 10 is the current density generated by electrons.

$$\frac{\partial n_p}{\partial t} + \nabla \cdot (n_p u_p) = 0 \quad \text{(Equation 4)}$$

$$m_e n_p \left\{ \frac{\partial}{\partial t} + u_p \cdot \nabla \right\} u_p = -en_p(E + u_p \times B) \quad \text{(Equation 5)}$$

$$\frac{\partial n_b}{\partial t} + \nabla \cdot (n_b u_b) = 0 \quad \text{(Equation 6)}$$

$$\gamma_0 m_e \left\{ \frac{\partial}{\partial t} + u_b \cdot \nabla \right\} u_b + m_e u_b \frac{\partial \gamma_1}{\partial t} = -e(E + u_b \times B) \quad \text{(Equation 7)}$$

$$\nabla \times \vec{E}_i = -\frac{\partial \vec{B}_i}{\partial t} \quad \text{(Equation 8)}$$

$$\nabla \times \vec{B}_i = \mu_0 J + \frac{1}{C^2} \frac{\partial \vec{E}_i}{\partial t} \quad \text{(Equation 9)}$$

$$J = \left(-en_{b0}u_{bz} - en_{b1}u_{b0z} - en_{p0}u_{ez} \right)\vec{z} + \left(-en_{p0}u_{ey} - en_{b0}u_{by} \right)\vec{y} \quad \text{(Equation 10)}$$

Where n_p is the plasma electron density; n_b is the electron beam density; u_p is the plasma electron velocity; u_b is the electron beam velocity; m_e is the electronic quality; γ is the relativistic factor, $\gamma = 1/\sqrt{1 - u_b^2/C^2}$ and C is speed of light, because the speed of the electron beam is in the following form: $u_b = u_{b0z} + u_{b1}$, the relativistic factor can therefore also be expanded as follows: $\gamma = \gamma_0 + \gamma_1 + R_n(u_{b1})$, γ_1 is a first-order Taylor expansion at position u_{b1}; $R_n(u_{b1})$ is a high-order infinitesimal; E is the induced electric field; B is is the total magnetic induction, including the magnetic field generated by the electron beam B_b and the induced magnetic field B_1.

According to Ampere's loop law, the magnetic field in the electron beam is

$$B_b = -\mu_0 en_{b0}u_{b0}y / 2 (y \le y_0) \quad \text{(Equation 11)}$$

Where y_0 represents the boundary of the electron beam or the thickness of the electron beam. The derivative of y with respect to time can be expressed as

$$\frac{dy}{dt} = \left(\frac{\partial}{\partial t} + u_{b0} \frac{\partial}{\partial z} \right) y = -i\omega + ik_z u_{b0} = u_{by} \quad \text{(Equation 12)}$$

Inside the electron beam, the magnetic field generated by the electron beam is

$$B_b = \frac{\mu_0 en_{b0}u_{b0}}{2i(\omega - k_z u_{b0})} u_{by} \quad \text{(Equation 13)}$$

Therefore, inside the electron beam, $u_{b1} \times B_b$ is a higher order small quantity and can be ignored. Within the electron beam, the influence of the x-direction magnetic field generated by the electron beam itself is ignored, while outside the electron beam (at the plasma), the magnetic field generated by the electron beam is not ignored.

For the middle term of Equation 7

$$m_e u_b \frac{\partial \gamma_1}{\partial t} = \frac{u_b}{C^2} \frac{d\left(\gamma m_e C^2\right)}{dt} = \frac{u_b}{C^2} \frac{dW}{dt} \quad \text{(Equation 14)}$$

W is the energy of an electron. Because

$$\frac{dW}{dt} = F \cdot u_b = e(E + u_b \times B) \cdot u_b \quad \text{(Equation 15)}$$

Substituting Equations 15 and 14 into Equation 7, we obtained

$$\gamma_0 m_e \left\{ \frac{\partial}{\partial t} + u_b \cdot \nabla \right\} u_b + \frac{u_b}{C^2} eE \cdot u_b = -e(E + u_b \times B) \quad \text{(Equation 16)}$$

Using perturbation method to linearize Equations 4, 5, 6, 7, 8, 9, and 10, ignoring high-order small quantities above 2nd order, derived from Equations 4 and 6, we obtained:

$$\begin{cases} -\omega n_{p1} + k_y n_{p0} u_{ey} + k_z n_{p0} u_{ez} = 0 \\ (k_z u_{b0z} - \omega) n_{b1} + k_y n_{b0} u_{by} + k_z n_{b0} u_{bz} = 0 \end{cases} \quad \text{(Equation 17)}$$

After linearizing Equation 5, it is obtained that:

$$\begin{cases} u_{py} = \dfrac{1}{\left[1 + \left(\dfrac{eB_t}{i\omega m_e}\right)^2\right]} \dfrac{e}{i\omega m_e} E_y + \dfrac{1}{\left[1 + \left(\dfrac{eB_t}{i\omega m_e}\right)^2\right]} \left(\dfrac{e}{i\omega m_e}\right)^2 B_t E_z \\ u_{pz} = \dfrac{1}{\left[1 + \left(\dfrac{eB_t}{i\omega m_e}\right)^2\right]} \dfrac{e}{i\omega m_e} E_z - \dfrac{1}{\left[1 + \left(\dfrac{eB_t}{i\omega m_e}\right)^2\right]} \left(\dfrac{e}{i\omega m_e}\right)^2 B_t E_y \end{cases} \quad \text{(Equation 18)}$$

Where B_t is the superposition of the x-direction magnetic field B_b generated by the electron beam in the plasma and the uniformly applied magnetic field B_0 externally: $B_t = B_b + B_0$. Linearize Equation 16 and use the first term of Equation 19 to obtain

$$\begin{cases} u_{by} = \left(\dfrac{C_1}{\left[1 + C_1^2 B_{0x}^2\right]} - \dfrac{k_z}{\omega} \dfrac{C_1 u_{b0z}}{\left[1 + C_1^2 B_{0x}^2\right]} \right) E_y + \dfrac{C_1^2 B_{0x}}{\left[1 + C_1^2 B_{0x}^2\right]} \left(1 + \dfrac{u_{b0z}^2}{C^2}\right) E_z + \dfrac{k_y}{\omega} \dfrac{C_1 u_{b0z}}{\left[1 + C_1^2 B_{0x}^2\right]} E_z \\ u_{bz} = \dfrac{C_1}{\left[1 + C_1^2 B_{0x}^2\right]} \left(1 + \dfrac{u_{b0z}^2}{C^2}\right) E_z + \left[\dfrac{k_z}{\omega} \dfrac{C_1^2 u_{b0z} B_{0x}}{\left[1 + C_1^2 B_{0x}^2\right]} - \dfrac{C_1^2 B_{0x}}{\left[1 + C_1^2 B_{0x}^2\right]} \right] E_y - \dfrac{k_y}{\omega} \dfrac{C_1^2 u_{b0z} B_{0x}}{\left[1 + C_1^2 B_{0x}^2\right]} E_z \end{cases} \quad \text{(Equation 19)}$$

Where

$$C_1 = \frac{e}{\gamma_0 m_e (i\omega - i k_z u_{b0z})} \quad \text{(Equation 20)}$$

Bringing Equation 19 into the second equation of Equation 17, we obtain

$$n_{b1} = D_2 E_y + D_3 E_z \quad \text{(Equation 21)}$$

Where

$$\begin{cases} D_2 = \dfrac{1}{(\omega - k_z u_{b0z})} \left\{ k_y n_{b0} \left(\dfrac{C_1}{\left[1 + C_1^2 B_{0x}^2\right]} - \dfrac{k_z}{\omega} \dfrac{C_1 u_{b0z}}{\left[1 + C_1^2 B_{0x}^2\right]} \right) + k_z n_{b0} \left[\dfrac{k_z}{\omega} \dfrac{C_1^2 u_{b0z} B_{0x}}{\left[1 + C_1^2 B_{0x}^2\right]} - \dfrac{C_1^2 B_{0x}}{\left[1 + C_1^2 B_{0x}^2\right]} \right] \right\} \\ D_3 = \dfrac{1}{(\omega - k_z u_{b0z})} \left\{ k_z n_{b0} \left[\dfrac{C_1}{\left[1 + C_1^2 B_{0x}^2\right]} \left(1 + \dfrac{u_{b0z}^2}{C^2}\right) - \dfrac{k_y}{\omega} \dfrac{C_1^2 u_{b0z} B_{0x}}{\left[1 + C_1^2 B_{0x}^2\right]} \right] \right. \\ \left. + k_y n_{b0} \left[\dfrac{C_1^2 B_{0x}}{\left[1 + C_1^2 B_{0x}^2\right]} \left(1 + \dfrac{u_{b0z}^2}{C^2}\right) + \dfrac{k_y}{\omega} \dfrac{C_1 u_{b0z}}{\left[1 + C_1^2 B_{0x}^2\right]} \right] \right\} \end{cases} \quad \text{(Equation 22)}$$

Linearizing Equations 8, 9, and 10, it is obtained that:

$$\begin{cases} k_y E_{1z} - k_z E_{1y} - \omega B_{1x} = 0 \\ n_{b0} u_{by} + n_{p0} u_{ey} + i\omega E_{1y} / \mu_0 e C^2 + i k_z B_{1x} / \mu_0 e = 0 \\ n_{b1} u_{b0z} + n_{b0} u_{bz} + n_{p0} u_{ez} + i\omega E_{1z} / \mu_0 e C^2 - i k_y B_{1x} / \mu_0 e = 0 \end{cases} \quad \text{(Equation 23)}$$

Bringing Equations 18, 19, and 21 and first equation of Equation 23 into the second and third equations of Equation 23, we obtain

$$\begin{cases} AE_y + BE_z = 0 \\ CE_y + DE_z = 0 \end{cases} \quad \text{(Equation 24)}$$

$$C_1 = \frac{e}{i\gamma_0 m_e \omega_{be}(\Omega - Z)} \quad \text{(Equation 29)}$$

Where

$$\begin{cases} A_{11} = n_{b0}\left(\frac{C_1}{\left[1+C_1^2B_{0x}^2\right]} - \frac{k_z}{\omega}\frac{C_1 u_{b0z}}{\left[1+C_1^2B_{0x}^2\right]}\right) + n_{p0}\frac{1}{\left[1+\left(\frac{eB_t}{i\omega m_e}\right)^2\right]}\frac{e}{i\omega m_e} + \frac{i\omega}{\mu_0 e C^2} - \frac{ik_z}{\mu_0 e}\frac{k_z}{\omega} \\ A_{12} = n_{b0}\left[\frac{C_1^2 B_{0x}}{\left[1+C_1^2B_{0x}^2\right]}\left(1+\frac{u_{b0z}^2}{C^2}\right) + \frac{k_y}{\omega}\frac{C_1 u_{b0z}}{\left[1+C_1^2B_{0x}^2\right]}\right] + n_{p0}\frac{1}{\left[1+\left(\frac{eB_t}{i\omega m_e}\right)^2\right]}\left(\frac{e}{i\omega m_e}\right)^2 B_t + \frac{ik_z}{\mu_0 e}\frac{k_y}{\omega} \\ A_{21} = D_2 u_{b0z} - \frac{n_{p0}}{\left[1+\left(\frac{eB_t}{i\omega m_e}\right)^2\right]}\left(\frac{e}{i\omega m_e}\right)^2 B_t + n_{b0}\left[\frac{k_z}{\omega}\frac{C_1^2 u_{b0z} B_{0x}}{\left[1+C_1^2B_{0x}^2\right]} - \frac{C_1^2 B_{0x}}{\left[1+C_1^2B_{0x}^2\right]}\right] + \frac{ik_y}{\mu_0 e}\frac{k_z}{\omega} \\ A_{22} = D_3 u_{b0z} + \frac{n_{b0}C_1}{\left[1+C_1^2B_{0x}^2\right]}\left(1+\frac{u_{b0z}^2}{C^2}\right) - n_{b0}\frac{k_y}{\omega}\frac{C_1^2 u_{b0z} B_{0x}}{\left[1+C_1^2B_{0x}^2\right]} + \frac{n_{p0}}{\left[1+\left(\frac{eB_t}{i\omega m_e}\right)^2\right]}\frac{e}{i\omega m_e} + \frac{i\omega}{\mu_0 e C^2} - \frac{ik_y}{\mu_0 e}\frac{k_y}{\omega} \end{cases} \quad \text{(Equation 25)}$$

In order to satisfy that the aforementioned Equation 25 have non-zero solutions, the determinant coefficient of the equations must be 0.

$$\begin{vmatrix} A_{11} & A_{12} \\ A_{21} & A_{22} \end{vmatrix} = 0 \quad \text{(Equation 26)}$$

When analyzing the dispersion relationship between w and k, we first normalize the dispersion relationship of Equation 26, as shown in the following text:

$$\begin{cases} \omega_{bce} = \frac{eB_b}{m_e} \\ \omega_{ce0} = \frac{eB_{0x}}{m_e} \\ \omega_{be}^2 = \frac{e^2 n_{b0}}{\varepsilon_0 m_e} \end{cases} \quad \text{(Equation 27)}$$

and

$$\begin{cases} \omega_{pe}^2 = \frac{e^2 n_{p0}}{\varepsilon_0 m_e} \\ \Omega = \frac{\omega}{\omega_{be}} \\ Z = k_z \frac{u_{b0z}}{\omega_{be}} \end{cases} \quad \text{(Equation 28)}$$

Substituting Equations 27 and 28 into Equations 20, 22, and 25,we obtained

$$D_2 = \left[-i\frac{Z}{\Omega}\frac{1}{\gamma_0(\Omega - Z)} + \frac{\omega_{ce0}}{\omega_{be}}\frac{Z}{\Omega}\left(\frac{1}{\gamma_0(\Omega - Z)}\right)^2\right] \times \frac{1}{\left[1-\left(\frac{\omega_{ce0}}{\gamma_0\omega_{be}(\Omega - Z)}\right)^2\right]}\frac{1}{u_{b0z}}\frac{\varepsilon_0}{e}\omega_{be} \quad \text{(Equation 30)}$$

$$D_3\left[= i\frac{\left[-1-\frac{u_{b0z}^2}{C^2}-\frac{Z}{\Omega}\right]\left(\frac{Z}{\gamma_0(\Omega - Z)^2}\right)}{\left[1-\left(\frac{\omega_{ce0}}{\gamma_0\omega_{be}(\Omega - Z)}\right)^2\right]} + \frac{Z}{(\Omega - Z)}\frac{\omega_{be}}{\omega_{ce0}} \times \frac{\left[\frac{Z}{\Omega}-1-\frac{u_{b0z}^2}{C^2}\right]\left(\frac{\omega_{ce0}}{\gamma_0\omega_{be}(\Omega - Z)}\right)^2}{\left[1-\left(\frac{\omega_{ce0}}{\gamma_0\omega_{be}(\Omega - Z)}\right)^2\right]}\right]\frac{1}{u_{b0z}}\frac{\varepsilon_0}{e}\omega_{be} \quad \text{(Equation 31)}$$

$$A_{11} = i\left(\frac{Z}{\Omega}-1\right)\frac{\gamma_0(\Omega - Z)}{(\gamma_0(\Omega - Z))^2 - \frac{\omega_{ce0}^2}{\omega_{be}^2}}\frac{\varepsilon_0}{e}\omega_{be} - i\frac{1}{\left[1-\left(\frac{\omega_{bce}+\omega_{ce0}}{\omega_{be}}\right)^2\frac{1}{\Omega^2}\right]}\frac{\omega_{pe}^2}{\omega_{be}^2\Omega}\frac{\varepsilon_0}{e}\omega_{be} + i\left(\Omega - \frac{C^2}{u_{b0z}^2}\frac{Z^2}{\Omega}\right)\frac{\varepsilon_0}{e}\omega_{be} \quad \text{(Equation 32)}$$

$$A_{12} = \frac{-\left(\frac{\omega_{ce0}}{\gamma_0\omega_{be}(\Omega - Z)}\right)^2}{\left[1 - \left(\frac{\omega_{ce0}}{\gamma_0\omega_{be}(\Omega - Z)}\right)^2\right]}\left(1 + \frac{u_{b0z}^2}{C^2}\right)\frac{\omega_{be}}{\omega_{ce0}}\frac{\varepsilon_0}{e}\omega_{be} - \frac{\left(\frac{\omega_{bce} + \omega_{ce0}}{\omega_{be}\Omega}\right)^2}{\left[1 - \left(\frac{\omega_{bce} + \omega_{ce0}}{\omega_{be}\Omega}\right)^2\right]}\frac{\omega_{pe}^2}{\omega_{be}(\omega_{bce} + \omega_{ce0})}\frac{\varepsilon_0}{e}\omega_{be} - i\frac{\frac{\omega_{ce0}}{\gamma_0\omega_{be}(\Omega - Z)}}{\left[1 - \left(\frac{\omega_{ce0}}{\gamma_0\omega_{be}(\Omega - Z)}\right)^2\right]}\frac{Z}{\Omega}\frac{\omega_{be}}{\omega_{ce0}}\frac{\varepsilon_0}{e}\omega_{be} + i\frac{C^2}{u_{b0z}^2}\frac{Z^2}{\Omega}\frac{\varepsilon_0}{e}\omega_{be}$$

(Equation 33)

$$A_{21} = -i\frac{Z}{\Omega}\frac{1}{\gamma_0(\Omega - Z)}\frac{1}{\left[1 - \left(\frac{\omega_{ce0}}{\gamma_0\omega_{be}(\Omega - Z)}\right)^2\right]}\frac{\varepsilon_0}{e}\omega_{be} + \frac{\omega_{ce0}}{\omega_{be}}\frac{Z}{\Omega}\left(\frac{1}{\gamma_0(\Omega - Z)}\right)^2\frac{1}{\left[1 - \left(\frac{\omega_{ce0}}{\gamma_0\omega_{be}(\Omega - Z)}\right)^2\right]} \times \frac{\varepsilon_0}{e}\omega_{be} + \frac{\omega_{pe}^2}{\omega_{be}(\omega_{bce} + \omega_{ce0})}\frac{1}{\left[\Omega^2 - \left(\frac{\omega_{bce} + \omega_{ce0}}{\omega_{be}}\right)^2\right]} \times \left(\frac{\omega_{bce} + \omega_{ce0}}{\omega_{be}}\right)^2\frac{\varepsilon_0}{e}\omega_{be} + i\frac{C^2}{u_{b0z}^2}\frac{Z^2}{\Omega}\frac{\varepsilon_0}{e}\omega_{be} - \frac{\omega_{be}}{\omega_{ce0}}\left(\frac{Z}{\Omega} - 1\right) \times \left(\frac{\omega_{ce0}}{\gamma_0\omega_{be}(\Omega - Z)}\right)^2\frac{1}{\left[1 - \left(\frac{\omega_{ce0}}{\gamma_0\omega_{be}(\Omega - Z)}\right)^2\right]}\frac{\varepsilon_0}{e}\omega_{be}$$

(Equation 34)

$$A_{22} = \left[i\left(-1 - \frac{u_{b0z}^2}{C^2} - \frac{Z}{\Omega}\right)\left(\frac{Z}{\gamma_0(\Omega - Z)^2}\right) - i\frac{1 + \frac{u_{b0z}^2}{C^2}}{\gamma_0(\Omega - Z)}\right] \times \frac{1}{\left[1 - \left(\frac{\omega_{ce0}}{\gamma_0\omega_{be}(\Omega - Z)}\right)^2\right]}\frac{\varepsilon_0}{e}\omega_{be} + \left[\left(\frac{Z}{\Omega} - 1 - \frac{u_{b0z}^2}{C^2}\right) \times \frac{Z}{(\Omega - Z)} + \frac{Z}{\Omega}\right]\frac{\omega_{be}}{\omega_{ce0}}\frac{\left(\frac{\omega_{ce0}}{\gamma_0\omega_{be}(\Omega - Z)}\right)^2}{\left[1 - \left(\frac{\omega_{ce0}}{\gamma_0\omega_{be}(\Omega - Z)}\right)^2\right]}\frac{\varepsilon_0}{e}\omega_{be} - i\frac{1}{\Omega\left[1 - \frac{1}{\Omega^2}\left(\frac{\omega_{ce0} + \omega_{bce}}{\omega_{be}}\right)^2\right]}\frac{\omega_{pe}^2}{\omega_{be}^2}\frac{\varepsilon_0}{e}\omega_{be} + i\left[\Omega - \frac{C^2}{u_{b0z}^2}\frac{Z^2}{\Omega}\right]\frac{\varepsilon_0}{e}\omega_{be}$$

(Equation 35)

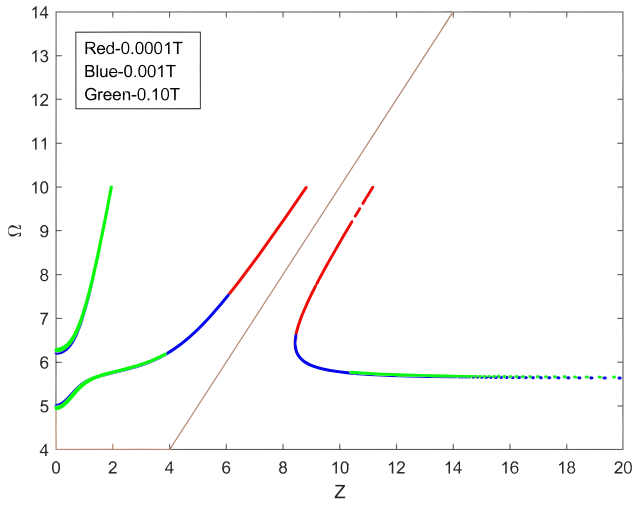

Figure 2. Dispersion curve under different magnetic field (perturbational method)

Figure 2 shows the dispersion curves obtained using perturbation method under different magnetic fields. Figure 2 shows that as the magnetic field increases, the radiation frequency and bandwidth of electromagnetic waves decrease accordingly.

By substituting Equations 32, 33, 34, and 35 into Equation 26, the dispersion relationship of microwave radiation generated by the interaction between the electron beam and the plasma under radial magnetization is obtained. Figure 2 shows the dispersion curves under the conditions of an electron beam velocity of $1*10^8$ m/s, a plasma density of $5\times10^{18}m^{-3}$, an electron beam electron density of $5*10^{17}m^{-3}$ and the transverse magnetic fields of 0.1T, 0.001T, and 0.0001T. The red area in the figure coincides with the blue and green areas, and the blue area coincides with the green area. Figure 2 shows that as the magnetic field increases, the radiation frequency and bandwidth of electromagnetic waves decrease accordingly. Figure 3 shows the dispersion curves under the conditions of a transverse magnetic field of 0.0001T, an electron beam velocity of $1*10^8$ m/s, an electron beam electron density of $5*10^{17}m^{-3}$, and plasma density of $3*10^{18}m^{-3}$, $5*10^{18}m^{-3}$, and $7*10^{18}m^{-3}$, respectively. Figure 4 shows the dispersion curves under the conditions of a transverse magnetic field of 0.0001T, an electron beam velocity of $1*10^8$ m/s, a plasma density of $8*10^{17}m^{-3}$, and an electron beam electron density of $5*10^{17}m^{-3}$, $1*10^{17}m^{-3}$, and $5*10^{16}m^{-3}$, respectively. The closer the electron beam electron density is to the plasma density, the larger the plasma radiation bandwidth. Figure 4 also indicates that when the electron density of the electron beam is low, the dispersion curve of radiation appears in a low-frequency region.

Figure 5 shows the dispersion curves under the conditions of a transverse magnetic field of 0.0001T, plasma density of $3*10^{18}m^{-3}$, electron beam electron density of $5*10^{17}m^{-3}$, and electron beam velocities of $1*10^7$ m/s, $5*10^7$ m/s, $1*10^8$ m/s, respectively. As the electron beam velocity increases, the radiation frequency, high-frequency region, and low-frequency region's radiation bandwidth all correspondingly increase.

The dispersion relationship derived using perturbation method is obtained under infinite plasma conditions, and this method cannot consider the boundary condition problem between plasma and

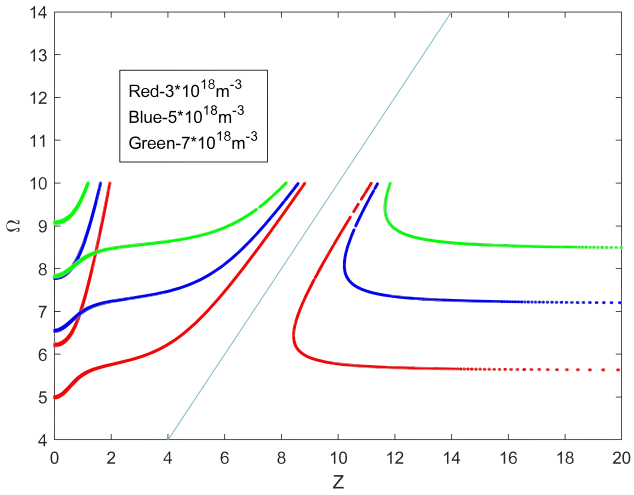

Figure 3. Dispersion curve under different plasma electron densities (perturbational method)

Figure 3 shows the dispersion curves obtained using perturbation method at different plasma densities.

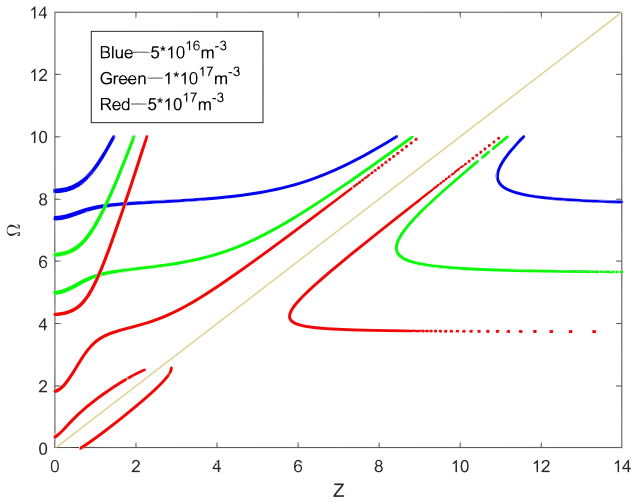

Figure 4. Dispersion curve under different electron beam electron densities (perturbational method)

Figure 4 shows the dispersion curves obtained using perturbation method at different electron beam electron densities. The closer the electron beam electron density is to the plasma density, the larger the plasma radiation bandwidth.

electron beam. In order to further obtain a more accurate dispersion relationship under the interaction between electron beam and transverse magnetized plasma, the field matching method is used to solve it.

Deduction of dispersion relationship-field-matching method

In the process of using field matching method to solve, considering the y-direction boundary conditions of plasma and electron beam, the disturbance quantity are transformed into the following form: $f_1 \propto \exp(ikz - i\omega t)$. Solve Equations 4 and 5, we obtained

$$n_{p1} = \frac{k_z n_{p0}}{\omega} u_{pz} - i\frac{n_{p0}}{\omega}\frac{\partial u_{py}}{\partial y} \quad \text{(Equation 36)}$$

$$u_{pz} = \frac{i\omega m_e}{e^2B_t^2 - \omega^2 m_e^2} eE_{pz} - \frac{eB_t}{e^2B_t^2 - \omega^2 m_e^2} eE_{py} \quad \text{(Equation 37)}$$

$$u_{py} = \frac{eB_t}{e^2B_t^2 - \omega^2 m_e^2} eE_{pz} + \frac{i\omega m_e}{e^2B_t^2 - \omega^2 m_e^2} eE_{py} \quad \text{(Equation 38)}$$

Comparing the real and imaginary parts in Equations 37 and 38. Regarding the observations made in the experiment, there are $\omega > \omega_{be} \approx \omega_{pe}$. When the electron beam speed is 0.6*C*, the electron beam radius *R* is *1*cm, and the electron beam current is *1*kA, the $\frac{\omega_{ce}}{\omega_{be}} = \sqrt{\frac{e^2\mu_0 C}{4m_e}}\gamma R\sqrt{n_{b0}} \approx 0.1$, so $\omega \gg \omega_{ce}$. From the analysis results of perturbation method, it is found that the larger the transverse magnetic field, the less obvious the electromagnetic wave radiation. Therefore, the applied transverse magnetic field is smaller, and the cyclotron frequency generated by the applied magnetic field and the magnetic field caused by the electron beam is much lower than the microwave radiation frequency.

$$\frac{\frac{i\omega m_e}{e^2B_t^2 - \omega^2 m_e^2} eE_{pz}}{\frac{eB_t}{e^2B_t^2 - \omega^2 m_e^2} eE_{py}} = \frac{\omega}{\omega_{ce}} \tan\theta \quad \text{(Equation 39)}$$

θ is the radiation angle of electromagnetic waves. In the experiment, it was measured that θ is 43°–48°, $\tan\theta \approx 1$. Therefore, the plasma velocity disturbance only needs to retain the imaginary part. Using Equation 10, we obtained

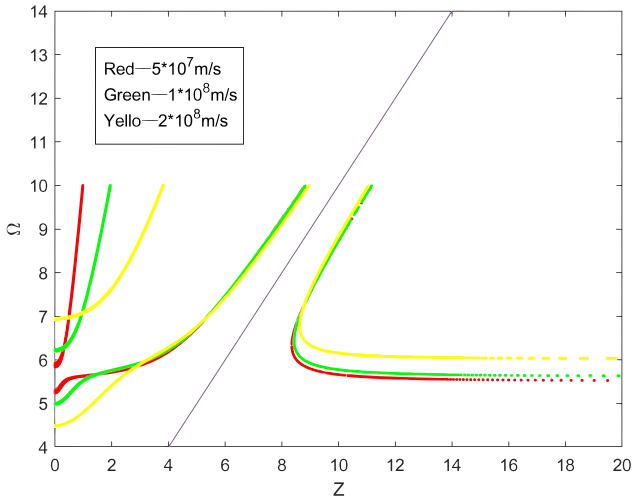

Figure 5. Dispersion curve under different electron beam velocity (perturbational method)

Figure 5 shows the dispersion curves obtained using perturbation method at different electron beam velocity. As the electron beam velocity increases, the radiation frequency, high-frequency region, and low-frequency region's radiation bandwidth all correspondingly increase.

$$J_{py} = -\frac{ie\omega m_e}{e^2B_t^2 - \omega^2 m_e^2} en_{p0}E_{py} \quad \text{(Equation 40)}$$

$$J_{pz} = -\frac{ie\omega m_e}{e^2B_t^2 - \omega^2 m_e^2} en_{p0}E_{pz} \quad \text{(Equation 41)}$$

Solve Equations 6 and 16, we obtained

$$n_{b1} = \frac{n_{b0}}{\omega - ku_{b0z}} k_z u_{bz} - i\frac{n_{b0}}{\omega - ku_{b0z}}\frac{\partial u_{by}}{\partial y} \quad \text{(Equation 42)}$$

$$u_{by} = \frac{C_1}{\left[1 + C_1^2B_{0x}^2\right]}E_{by} + \frac{C_1^2B_{0x}}{\left[1 + C_1^2B_{0x}^2\right]}\left(1 + \frac{u_{b0z}^2}{C^2}\right)E_z + \frac{C_1u_{b0z}}{\left[1 + C_1^2B_{0x}^2\right]}B_{1x} \quad \text{(Equation 43)}$$

$$u_{bz} = \frac{C_1}{\left[1 + C_1^2B_{0x}^2\right]}\left(1 + \frac{u_{b0z}^2}{C^2}\right)E_z - \frac{C_1^2B_{0x}}{\left[1 + C_1^2B_{0x}^2\right]}E_{by} - \frac{C_1^2u_{b0z}B_{0x}}{\left[1 + C_1^2B_{0x}^2\right]}B_{1x} \quad \text{(Equation 44)}$$

The relationship in the electromagnetic field is as follows:

$$\nabla \times E = \frac{\partial E_{bz}}{\partial y} - \frac{\partial E_{by}}{\partial z} = -\frac{\partial B_{bx}}{\partial t} = i\omega B_{bx} \Rightarrow B_{bx} = \frac{1}{i\omega}\left(\frac{\partial E_{bz}}{\partial y} - \frac{\partial E_{by}}{\partial z}\right) \quad \text{(Equation 45)}$$

We obtained

$$u_{by} = \left(\frac{C_1}{\left[1 + C_1^2B_{0x}^2\right]} - \frac{k_z}{\omega}\frac{C_1u_{b0z}}{\left[1 + C_1^2B_{0x}^2\right]}\right)E_{by} + \frac{C_1^2B_{0x}}{\left[1 + C_1^2B_{0x}^2\right]}\left(1 + \frac{u_{b0z}^2}{C^2}\right)E_{bz} + \frac{1}{i\omega}\frac{C_1u_{b0z}}{\left[1 + C_1^2B_{0x}^2\right]}\frac{\partial E_{bz}}{\partial y} \quad \text{(Equation 46)}$$

$$u_{bz} = \frac{C_1}{\left[1 + C_1^2B_{0x}^2\right]}\left(1 + \frac{u_{b0z}^2}{C^2}\right)E_{bz} + \left[\frac{k_z}{\omega}\frac{C_1^2u_{b0z}B_{0x}}{\left[1 + C_1^2B_{0x}^2\right]} - \frac{C_1^2B_{0x}}{\left[1 + C_1^2B_{0x}^2\right]}\right]E_{by} - \frac{1}{i\omega}\frac{C_1^2u_{b0z}B_{0x}}{\left[1 + C_1^2B_{0x}^2\right]}\frac{\partial E_{bz}}{\partial y} \quad \text{(Equation 47)}$$

According to the aforementioned analysis, when the external magnetic field is weak, Equations 1 and 2 are approximately in the following form :

$$u_{by} = \left(\frac{C_1}{\left[1 + C_1^2B_{0x}^2\right]} - \frac{k_z}{\omega}\frac{C_1u_{b0z}}{\left[1 + C_1^2B_{0x}^2\right]}\right)E_{by} + \frac{1}{i\omega}\frac{C_1u_{b0z}}{\left[1 + C_1^2B_{0x}^2\right]}\frac{\partial E_{bz}}{\partial y} \quad \text{(Equation 48)}$$

$$u_{bz} = \frac{C_1}{\left[1 + C_1^2B_{0x}^2\right]}\left(1 + \frac{u_{b0z}^2}{C^2}\right)E_{bz} \quad \text{(Equation 49)}$$

Using Equation 10, we obtained

$$J_{bz} = C_2E_{bz} + C_3\frac{\partial E_{by}}{\partial y} + C_4\frac{\partial^2 E_{bz}}{\partial y^2} \quad \text{(Equation 50)}$$

$$J_{by} = C_5E_{by} + C_6\frac{\partial E_{bz}}{\partial y} \quad \text{(Equation 51)}$$

Where

$$\begin{cases} C_2 = \left[-1 - \frac{k_zu_{b0z}}{\omega - ku_{b0z}}\right]\frac{en_{b0}C_1}{\left[1 + C_1^2B_{0x}^2\right]}\left(1 + \frac{u_{b0z}^2}{C^2}\right) \\ C_3 = i\frac{eu_{b0z}n_{b0}}{\omega - ku_{b0z}}\left(\frac{C_1}{\left[1 + C_1^2B_{0x}^2\right]} - \frac{k_z}{\omega}\frac{C_1u_{b0z}}{\left[1 + C_1^2B_{0x}^2\right]}\right) \\ C_4 = \frac{eu_{b0z}n_{b0}}{\omega - ku_{b0z}}\frac{1}{\omega}\frac{C_1u_{b0z}}{\left[1 + C_1^2B_{0x}^2\right]} \\ C_5 = \frac{-en_{b0}C_1}{\left[1 + C_1^2B_{0x}^2\right]}\left(1 - \frac{k_zu_{b0z}}{\omega}\right) \\ C_6 = i\frac{u_{b0z}}{\omega}\frac{en_{b0}C_1}{\left[1 + C_1^2B_{0x}^2\right]} \end{cases} \quad \text{(Equation 52)}$$

Using Equations 8 and 9, obtain the wave equation for the field:

$$-\nabla \times (\nabla \times E) + \frac{\omega^2}{C^2}E = -i\omega\mu_0 J \quad \text{(Equation 53)}$$

Equation 53 can be decomposed into two directions of y and z.

$$-\frac{\omega^2}{C^2}E_y - i\omega\mu_0J_y = \frac{\partial}{\partial z}\left(\frac{\partial E_z}{\partial y} - \frac{\partial E_y}{\partial z}\right) \quad \text{(Equation 54)}$$

$$-\frac{\omega^2}{C^2}E_z - i\omega\mu_0J_z = -\frac{\partial}{\partial y}\left(\frac{\partial E_z}{\partial y} - \frac{\partial E_y}{\partial z}\right) \quad \text{(Equation 55)}$$

Bring Equation 40 into Equation 54, we obtain

$$i\left(\frac{\omega}{k_z}\frac{\omega}{C^2} + \frac{\omega}{k_z}\frac{e\omega\mu_0m_e}{e^2B_t^2 - \omega^2m_e^2}en_{p0} + k_z\right)E_{py} = \frac{\partial E_{pz}}{\partial y} \quad \text{(Equation 56)}$$

Bring Equation 41 into Equation 55, and using Equation 56, we obtain

$$\frac{\partial^2 E_{pz}}{\partial y^2} - \left(\frac{\omega^2}{C^2} + \frac{e\omega^2\mu_0 m_e}{e^2 B_t^2 - \omega^2 m_e^2} e n_{p0} + k_z^2\right) E_{pz} = 0 \quad \text{(Equation 57)}$$

Solve Equation 57

$$E_{pz} = f_1 \exp(py) + f_2 \exp(-py) \quad \text{(Equation 58)}$$

Where

$$p^2 = \frac{\omega^2}{C^2} + \frac{e\omega^2\mu_0 m_e}{e^2 B_t^2 - \omega^2 m_e^2} e n_{p0} + k_z^2 \quad \text{(Equation 59)}$$

Bring Equation 58 into Equation 56, we obtain

$$E_{py} = C_7 f_1 \exp(py) - C_7 f_2 \exp(-py) \quad \text{(Equation 60)}$$

Where

$$C_7 = \frac{p}{i\left(\frac{\omega}{k_z}\frac{\omega}{C^2} + \frac{\omega}{k_z}\frac{e\omega\mu_0 m_e}{e^2 B_t^2 - \omega^2 m_e^2} e n_{p0} + k_z\right)} \quad \text{(Equation 61)}$$

Bring Equation 51 into Equation 54, we obtain

$$\left(-\frac{\frac{\omega^2}{C^2} + i\omega\mu_0 C_5 + k_z^2}{ik_z + i\omega\mu_0 C_6}\right) E_{by} = \frac{\partial E_{bz}}{\partial y} \quad \text{(Equation 62)}$$

Bring Equation 50 into Equation 55, and using Equation 62,we obtain

$$E_{by} = g_1 \exp(qy) + g_2 \exp(-qy) \quad \text{(Equation 63)}$$

Where

$$q^2 = \frac{\frac{\omega^2}{C^2} + i\omega\mu_0 C_2}{\frac{(\omega\mu_0 C_3 + k_z)(k_z + \omega\mu_0 C_6)}{\frac{\omega^2}{C^2} + i\omega\mu_0 C_5 + k_z^2} + i\omega\mu_0 C_4 - 1} \quad \text{(Equation 64)}$$

Bring Equation 63 into Equation 62, we obtain

$$E_{bz} = C_8 g_1 \exp(qy) - C_8 g_2 \exp(-qy) \quad \text{(Equation 65)}$$

Where

$$C_8 = -\frac{\frac{\omega^2}{C^2} + i\omega\mu_0 C_5 + k_z^2}{q(ik_z + i\omega\mu_0 C_6)} \quad \text{(Equation 66)}$$

Using the boundary conditions of electromagnetic field, the dispersion relation between electron beam and plasma with a transverse magnetic field can be obtained. At the boundary between electron beam and plasma, $y = y_0$ we obtain

$$B_{bx} = B_{px} \quad \text{(Equation 67)}$$

$$B_{bz} - B_{pz} = J_{py} + J_{by} \quad \text{(Equation 68)}$$

$$E_{bz} = E_{pz} \quad \text{(Equation 69)}$$

$$\int D \cdot ds = \int \delta\rho dV = -e \int n_1 dV \quad \text{(Equation 70)}$$

Using equation

$$\nabla \times E = \begin{pmatrix} \vec{x} & \vec{y} & \vec{z} \\ \frac{\partial}{\partial x} & \frac{\partial}{\partial y} & \frac{\partial}{\partial z} \\ 0 & E_y & E_z \end{pmatrix} = \left(\frac{\partial E_z}{\partial y} - \frac{\partial E_y}{\partial z}\right)\vec{x} + \left(-\frac{\partial E_z}{\partial x}\right)\vec{y} + \left(\frac{\partial E_y}{\partial x}\right)\vec{z} = i\omega B \quad \text{(Equation 71)}$$

Simultaneous Equation 58, 60, 63, 65 and 71, We obtain

$$B_z = 0 \quad \text{(Equation 72)}$$

$$B_{bx} = \frac{1}{i\omega}[C_8 q - ik_z]g_1 \exp(qy) + \frac{1}{i\omega}[C_8 q - ik_z]g_2 \exp(-qy) \quad \text{(Equation 73)}$$

$$B_{px} = \frac{1}{i\omega}[p - ik_z C_7]f_1 \exp(py) - \frac{1}{i\omega}[p - ik_z C_7]f_2 \exp(-py) \quad \text{(Equation 74)}$$

Using Equation 67, we obtained

$$[C_8 q - ik_z]g_1 \exp(qy_0) + [C_8 q - ik_z]g_2 \exp(-qy_0) - [p - ik_z C_7]f_1 \exp(py_0) + [p - ik_z C_7]f_2 \exp(-py_0) = 0 \quad \text{(Equation 75)}$$

Using Equations 40, 51, 60, 63, 65, 68 and 72, we obtained

$$-f_1\frac{ie^2\omega m_e n_{p0} C_7}{e^2 B_t^2 - \omega^2 m_e^2}\exp(py_0) + f_2\frac{ie^2\omega m_e n_{p0} C_7}{e^2 B_t^2 - \omega^2 m_e^2}\exp(-py_0) + g_1[C_5 + C_6 C_8 q]\exp(qy_0) + g_2[C_5 + C_6 C_8 q]\exp(-qy_0) = 0 \quad \text{(Equation 76)}$$

Using Equations 58 65 and 69, we obtained

$$f_1 \exp(py_0) + f_2 \exp(-py_0) - C_8 g_1 \exp(qy_0) + C_8 g_2 \exp(-qy_0) = 0 \quad \text{(Equation 77)}$$

The perturbation density n_1 (Equation 70) is the sum of perturbation densities n_{b1} and n_{p1} on both sides outside the electron beam and inside the electron beam, $n_1 = n_{b1} + n_{p1}$, using Equations 36 and 42

$$n_1 = -i\frac{n_{b0}}{\omega - ku_{b0z}}\frac{\partial u_{bz}}{\partial z} - i\frac{n_{b0}}{\omega - ku_{b0z}}\frac{\partial u_{by}}{\partial y} - i\frac{n_{p0}}{\omega}\frac{\partial u_{pz}}{\partial z} - i\frac{n_{p0}}{\omega}\frac{\partial u_{py}}{\partial y} \quad \text{(Equation 78)}$$

When $y \to y_0$ bring Equation 78 into Equation 70, we obtain

$$E_{by} - E_{py} = i\frac{en_{b0}}{\varepsilon_0(\omega - ku_{b0z})}u_{bz} + i\frac{en_{b0}}{\varepsilon_0(\omega - ku_{b0z})}u_{by} + i\frac{en_{p0}}{\varepsilon_0\omega}u_{pz} + i\frac{en_{p0}}{\varepsilon_0\omega}u_{py} \quad \text{(Equation 79)}$$

Using Equations 37, 38, 48, 49, 60, 63, and 79. we obtained

$$\left\{ i\frac{en_{b0}}{\varepsilon_0(\omega - ku_{b0z})}\frac{C_1}{\left[1 + C_1^2B_{0x}^2\right]}\left[\left(1 + \frac{u_{b0z}^2}{C^2}\right)C_8 + 1 + \frac{u_{b0z}}{\omega}C_8q - \frac{u_{b0z}k_z}{\omega}\right] - 1\right\}g_1\exp(qy_0) + \left\{ i\frac{en_{b0}}{\varepsilon_0(\omega - ku_{b0z})}\frac{C_1}{\left[1 + C_1^2B_{0x}^2\right]}\left[-\left(1 + \frac{u_{b0z}^2}{C^2}\right)C_8 + 1 + \frac{u_{b0z}}{\omega}C_8q - \frac{k_zu_{b0z}}{\omega}\right] - 1\right\}g_2\exp(-qy_0) + \left\{C_7 - [1 + C_7]\frac{e}{\varepsilon_0}\frac{em_en_{p0}}{e^2B_t^2 - \omega^2m_e^2}\right\}f_1\exp(py_0) - \left\{C_7 + [1 - C_7]\frac{e}{\varepsilon_0}\frac{em_en_{p0}}{e^2B_t^2 - \omega^2m_e^2}\right\}f_2\exp(-py_0) = 0 \quad \text{(Equation 80)}$$

Equations 75, 76, 77, and 80 constitute the boundary conditions for the interaction between an electron beam and a transverse magnetized plasma. To make the system of equations have non-zero solutions, the coefficient determinant is required to be 0, as follows

$$\begin{vmatrix} a_{11} & a_{12} & a_{13} & a_{14} \\ a_{21} & a_{22} & a_{23} & a_{24} \\ a_{31} & a_{32} & a_{33} & a_{34} \\ a_{41} & a_{42} & a_{43} & a_{44} \end{vmatrix} = 0 \quad \text{(Equation 81)}$$

Where

$$\begin{cases} a_{11} = -[p - ik_zC_7]\exp(py_0) \\ a_{12} = [p - ik_zC_7]\exp(-py_0) \\ a_{13} = [C_8q - ik_z]\exp(qy_0) \\ a_{14} = [C_8q - ik_z]\exp(-qy_0) \end{cases} \quad \text{(Equation 82)}$$

$$\begin{cases} a_{21} = -\frac{ie^2\omega m_en_{p0}C_7}{e^2B_t^2 - \omega^2m_e^2}\exp(py_0) \\ a_{22} = \frac{ie^2\omega m_en_{p0}C_7}{e^2B_t^2 - \omega^2m_e^2}\exp(-py_0) \\ a_{23} = [C_5 + C_6C_8q]\exp(qy_0) \\ a_{24} = [C_5 + C_6C_8q]\exp(-qy_0) \end{cases} \quad \text{(Equation 83)}$$

$$\begin{cases} a_{31} = \exp(py_0) \\ a_{32} = \exp(-py_0) \\ a_{33} = -C_8\exp(qy_0) \\ a_{34} = C_8\exp(-qy_0) \end{cases} \quad \text{(Equation 84)}$$

$$\begin{cases} a_{41} = \left\{C_7 - [1 + C_7]\frac{e}{\varepsilon_0}\frac{em_en_{p0}}{e^2B_t^2 - \omega^2m_e^2}\right\}\exp(py_0) \\ a_{42} = -\left\{C_7 + [1 - C_7]\frac{e}{\varepsilon_0}\frac{em_en_{p0}}{e^2B_t^2 - \omega^2m_e^2}\right\}\exp(-py_0) \\ a_{43} = \left\{i\frac{en_{b0}}{\varepsilon_0(\omega - ku_{b0z})}\frac{C_1}{\left[1 + C_1^2B_{0x}^2\right]}\left[\left(1 + \frac{u_{b0z}^2}{C^2}\right)C_8 + 1 + \frac{u_{b0z}}{\omega}C_8q - \frac{u_{b0z}k_z}{\omega}\right] - 1\right\}\exp(qy_0) \\ a_{44} = \left\{i\frac{en_{b0}}{\varepsilon_0(\omega - ku_{b0z})}\frac{C_1}{\left[1 + C_1^2B_{0x}^2\right]}\left[-\left(1 + \frac{u_{b0z}^2}{C^2}\right)C_8 + 1 + \frac{u_{b0z}}{\omega}C_8q - \frac{k_zu_{b0z}}{\omega}\right] - 1\right\}\exp(-qy_0) \end{cases} \quad \text{(Equation 85)}$$

Equation 81 is the dispersion relationship between the electron beam and the transverse magnetized plasma microwave radiation obtained under the field matching method. Figure 6 shows the dispersion curves generated under the conditions of plasma density of $1 \times 10^{15}m^{-3}$, electron beam density of $1.2 \times 10^{14}m^{-3}$, electron beam velocity of $2 \times 10^8m/s$, and transverse magnetic field of $B_{0x} = 0.3T, 0.1T, 0.05T, 0.00001T$, respectively. The white part in the Figure 6 represents the radiation area. When the transverse magnetic field is strong (Figure 6A),

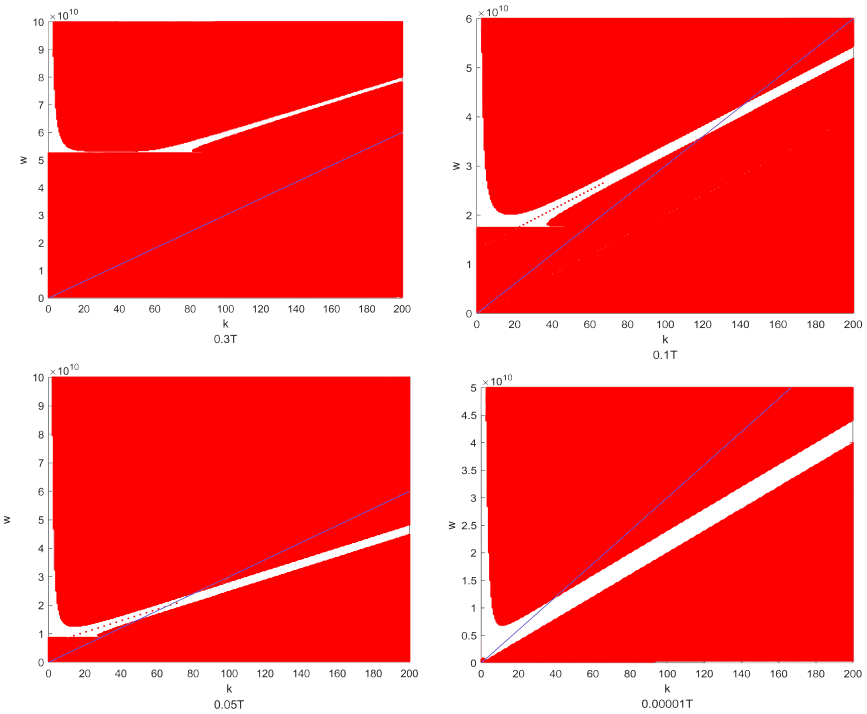

Figure 6. Dispersion curve under different magnetic field (field-matching method)

Dispersion curve obtained using field matching method under different magnetic field (white part and plasma density of $1 \times 10^{15}\ m^{-3}$, electron beam density of $1.2 \times 10^{14}\ m^{-3}$, electron beam velocity of $2 \times 10^{8}\ m/s$).

(A) 0.3T.

(B) 0.1T.

(C) 0.05T.

(D) 0.00001T.

the dispersion curve only occurs inside the plasma (to the left of the blue line). As the magnetic field weakens, the radiation bandwidth gradually increases (the width of the white area). Figure 7 shows the dispersion curves generated under the conditions of plasma density of $1 \times 10^{15} m^{-3}$, transverse magnetic field of $B_{0x} = 0.0001T$, electron beam velocity of $2 \times 10^{8} m/s$, and electron beam density of $n_{b0} = 0.4\times10^{14} m^{-3}, 1.2\times10^{14}\ m^{-3}, 2.0\times 10^{14} m^{-3}, 2.8\times10^{14} m^{-3}$ respectively. As the electron beam density approaches the plasma density, the radiation bandwidth significantly increases and the radiation frequency also increases according. Figure 8 shows the dispersion curves generated under the conditions of plasma density of $1 \times 10^{15} m^{-3}$, transverse magnetic field of $0.00001T$,electron beam density of $n_{b0} = 1.2\times10^{14} m^{-3}$ and electron beam velocity of $u_{b0z} = 0.1 \times 10^{8} m/s,\ 0.5 \times 10^{8} m/s,\ 1.0 \times 10^{8} m/s,\ 1.5 \times 10^{8} m/s$, respectively. As the electron beam density approaches the plasma density, the radiation bandwidth significantly increases and the radiation frequency also increases accordingly, but the change is not significant. As the electron beam velocity increases, the radiation frequency significantly increases, and the radiation bandwidth increases more significantly in the low-frequency region.

Comparison of simulation analysis results

The dispersion relationship is obtained through a set of magnetohydrodynamic equations. The interaction between electron beam and plasma is considered as two types of plasma interaction, and its mathematical model is composed of two sets of magnetohydrodynamic equations combined with Maxwell's equations (Equations 4, 5, 6, 7, 8, 9, and 10). In the aforementioned equation system, $n_p, u_p, n_b, u_b, E, B, J$ is the solving variable. The number of variables solved is equal to the number of equations. If simulation is used, the results obtained are the changes of each variable over time and space.

In order to further verify the correctness of the theoretical results, this paper uses MATLAB software to directly perform numerical calculations on the aforementioned equation system, and then compares the numerical calculation results with the theoretical derivation results.

Figure 9 shows the variation curve of the electric field over time under the conditions of electron beam velocity of 0.5C, electron beam density of 10^{16}cm^{-3}, magnetic field of 1mT, position of 0.05m, and plasma electron density of $1*10^{16}\text{cm}^{-3}$, $5*10^{16}\text{cm}^{-3}$, and $10*10^{16}\text{cm}^{-3}$, respectively. As the plasma density increases, the radiation frequency of the electric field also increases accordingly (The plasma densities are $1*10^{16}\text{cm}^{-3}$, $5*10^{16}\text{cm}^{-3}$, and $10*10^{16}\text{cm}^{-3}$ respectively, and the corresponding radiation frequency are 0.6 GHz, 1.01 GHz, and 1.47GHz), and the initial oscillation time of the plasma is delayed backwards with the increase of plasma density (The plasma densities are $1*10^{16}\text{cm}^{-3}$, $5*10^{16}\text{cm}^{-3}$, and $10*10^{16}\text{cm}^{-3}$ respectively, and the corresponding electric field onset oscillation times are 8.2 ns, 12.6 ns, and 14.8 ns). This indicates that under the condition of constant electron beam current, higher density plasma requires a longer time to excite the instability in the plasma. Figures 10 and 11 show the effects of different electron beam current densities on the radiation electric field. Figure 10 shows the variation curve of the electric field over time under the conditions of electron beam velocity of 0.5C, plasma electron density of $10*10^{16}\text{cm}^{-3}$, magnetic field of 1mT, position of 0.05m, and electron beam density of $1*10^{16}\text{cm}^{-3}$, $5*10^{16}\text{cm}^{-3}$, and $10*10^{16}\text{cm}^{-3}$, respectively. Figure 11 shows the variation curve of the electric field over time under the conditions of plasma electron density of $10*10^{16}\text{cm}^{-3}$, magnetic field of 1mT, position of 0.05 m, electron beam density of $10*10^{16}\text{cm}^{-3}$, and electron beam velocity of 0.5C, 0.6C, and 0.7C, respectively. Due to the interaction between the electron beam and the plasma, the electron beam converts some of its energy into the energy of electromagnetic waves. Therefore, an increase in the electron beam current (increasing the electron density or speed of

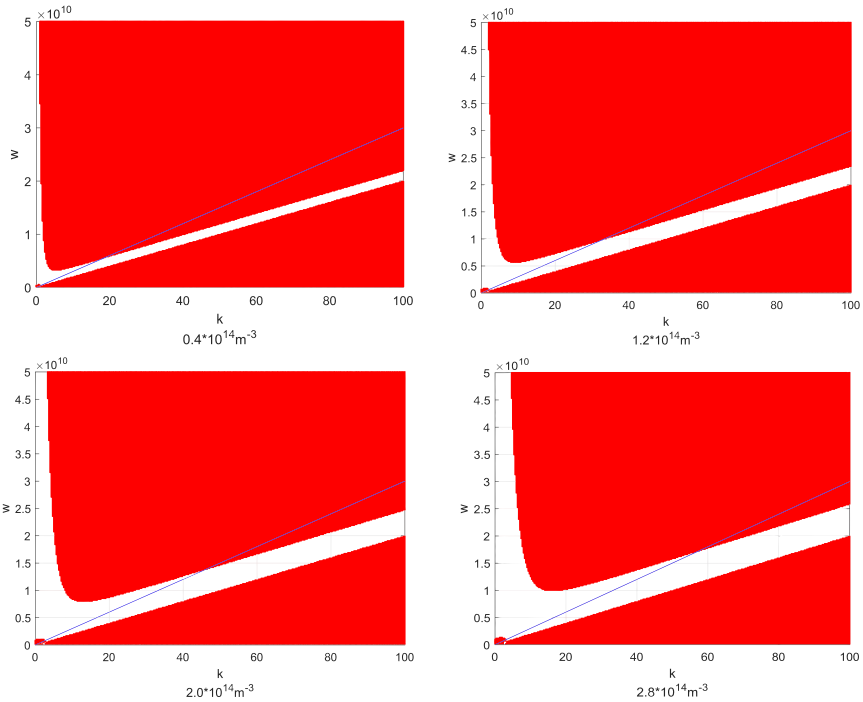

Figure 7. Dispersion curve under different electron beam densities (field-matching method)

Dispersion curve obtained using field matching method under different electron beam densities (plasma density of 1×10^{15} m^{-3}, transverse magnetic field of $B_{ox} = 0.0001T$, electron beam velocity of 2×10^8 m/s).

(A) 0.4×10^{14} m^{-3}.

(B) 1.2×10^{14} m^{-3}.

(C) 2.0×10^{14} m^{-3}.

(D) 2.8×10^{14} m^{-3}.

the electron beam) not only increases the radiation frequency of the electric field but also increases the radiation intensity of the electric field (In Figure 10, electron beam density are $1*10^{16}cm^{-3}$, $5*10^{16}cm^{-3}$, and $10*10^{16}cm^{-3}$, respectively, and the corresponding radiation frequency are 1.47 GHz, 3.1 GHz, and 6.2 GHz; in Figure 11, electron beam velocity are 0.5C, 0.6C, and 0.7C, respectively, and the corresponding radiation frequency are 1.47 GHz, 2.94 GHz, and 4.16 GHz). At the same time, the larger the electron beam current, the easier it is to excite electron oscillations in the plasma, resulting in a shorter initial oscillation time (In Figure 10, electron beam density are $1*10^{16}cm^{-3}$, $5*10^{16}cm^{-3}$, and $10*10^{16}cm^{-3}$, respectively, and the corresponding electric field onset oscillation times are 14.8 ns, 12.61 ns, and 10.1 ns; in the Figure 11, electron beam velocity are 0.5C, 0.6C, and 0.7C, respectively, and the corresponding electric field onset oscillation times are 14.8 ns, 12.02 ns, and 9.2 ns). Figure 12 shows the variation curve of the electric field over time under the conditions of electron beam velocity of 0.5C, plasma electron density of $1*10^{16}cm^{-3}$, electron beam density of $1*10^{16}cm^{-3}$, position of 0.05 m, and magnetic field of 1mT, 30mT, and 60mT, respectively. As the transverse magnetic field increases, the radiation frequency significantly increases (magnetic field are 1mT, 30mT, and 60mT, respectively, and the corresponding radiation frequency are 0.6 GHz, 1.31 GHz, and 5.56 GHz), but the initial oscillation time of the electric field is delayed (magnetic field are 1mT, 30mT, and 60mT, respectively, and the corresponding electric field onset oscillation times are 8.2 ns, 9.4 ns, and 11.1 ns) and the amplitude of the electric field is relatively weakened. When the electron beam passes through the plasma, the transverse magnetic field suppresses the oscillation between electrons, slows down the initial oscillation time of the electric field, and suppresses the propagation of electromagnetic waves. However, due to the increase in electron rotation frequency in the magnetic field, the overall radiation frequency of electromagnetic waves increases (this will be determined in subsequent analysis). This is consistent with the results in Figure 6 (as the magnetic field increases, the radiation frequency also increases but the radiation region [on the right side of the speed of light] narrows).

Result analysis and discussion

The second and third parts of this article provides a strict expression for the dispersion relationship (Equations 26 and 81 in the article), which not only considers the perturbations of plasma electron density and velocity but also the perturbations of electron beam electron density and velocity, making the dispersion relationship extremely complex and unable to further analyze the influence of various physical quantities on the dispersion relationship.

In early research, only the momentum conservation equation of plasma and Maxwell's equation (Equations 5, 8, 9, and 10) were usually considered. In order to further analyze the influence of various physical quantities on the dispersion relationship, a simple derivation of the dispersion relationship was carried out through Equations 5 and 7, 8, 9, and 10 (ignoring the perturbation of electron beam and plasma density, assuming that electron beam and plasma density are constant, i.e., ignoring Equations 4 and 6). Under the aforementioned conditions, a simple dispersion curve was derived (the derivation process is included in the appendix).

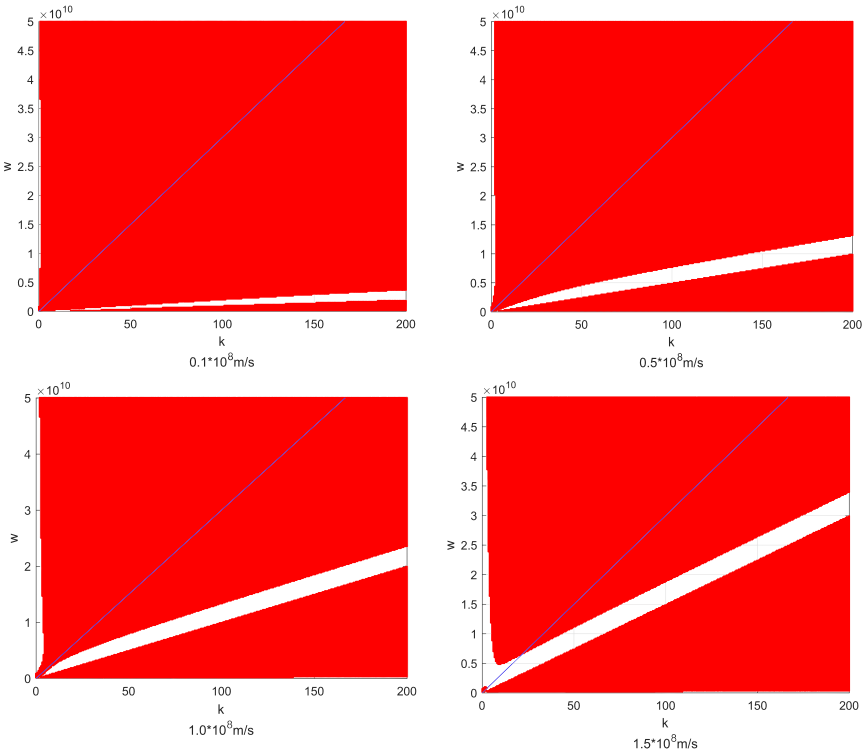

Figure 8. Dispersion curve under different electron beam velocity (field-matching method)

Dispersion curve obtained using field matching method under different electron beam velocity (plasma density of $1 \times 10^{15}\ m^{-3}$, transverse magnetic field of 0.00001T, electron beam density of $n_{b0} = 1.2 \times 10^{14}\ m^{-3}$).

(A) 0.1×10^8m/s.

(B) 0.5×10^8m/s.

(C) 1.0×10^8m/s.

(D) 1.5×10^8m/s.

$$n^2 = \frac{\left(\omega_{pe}^4 + \omega_{be}^4\right)\left[1 - \frac{\omega_{ce}^2}{\omega^2}\right] - 2\left(\omega^2 - \omega_{ce}^2\right)\omega_{pe}^2 + \left[\omega^2 - \omega_{ce}^2\right]^2 - \frac{2\omega_{pe}^2\omega_{be}^2\omega_{ce}^2}{\omega^2} + 2\omega_{pe}^2\omega_{be}^2}{2\left(\omega^2 - \omega_{ce}^2\right)\left[\omega^2 - \left(\omega_{ce}^2 + \omega_{pe}^2 + \omega_{be}^2\right)\right]} \quad \text{(Equation 86)}$$

Where

$n = \frac{kC}{\omega}$(Plasma refractive index).When $n = \infty$, the resonance point of the frequency can be determined, and the denominator is equal to zero, we obtain

$$\omega_{H1} = \omega_{ce} \text{ or } \omega_{H_2} = \sqrt{\omega_{ce}^2 + \omega_{be}^2 + \omega_{pe}^2} \quad \text{(Equation 87)}$$

$\omega_{H1}\omega_{H2}$ determines the upper limit of electromagnetic wave radiation frequency. From Equation 87, it can be seen that increasing the magnetic field intensity, electron beam density, or plasma density can all increase the radiation frequency. By increasing the magnetic field intensity, $\omega_{H2} - \omega_{H1}$ becomes relatively narrow (This conclusion is consistent with the conclusion in Figure 6), and increasing the plasma density and electron beam density can improve the radiation bandwidth. (This conclusion is consistent with the conclusion in Figure 7)

Applying a transverse magnetic field in a plasma not only magnetizes the plasma itself but also changes the trajectory of the electron beam. When the electron beam enters the plasma, it moves around the transverse magnetic field lines. On the one hand, this motion (swirling around magnetic field lines) constrains the range of motion of the electron beam in the plasma, reducing the interaction with the plasma in the z-direction. Therefore, the transverse magnetic field makes it difficult for electromagnetic waves to radiate from inside the plasma, as shown in Figures 2 and 6. On the other hand, the electron beam moves around the magnetic field lines, increasing the interaction time between the electron beam and the local plasma, making the interaction between the electron beam and the local plasma more complete. The electron beam also converts its own energy into microwaves more fully. Therefore, when the magnetic field is strong, its radiation frequency also increases accordingly, as shown in Figure 6. As the speed of the electron beam increases, the radius of the transverse magnetic field lines around the electron

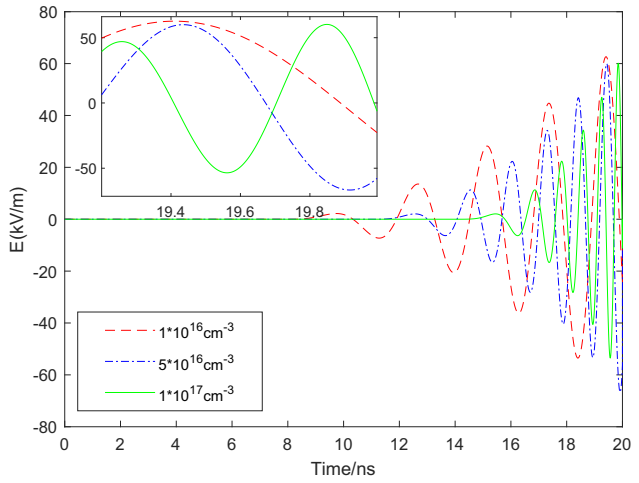

Figure 9. The variation curve of electric field over time (Different plasma electron densities)

Simulation analysis of electric field strength under different plasma densities. As the plasma density increases, the radiation frequency of the electric field also increases accordingly, and the initial oscillation time of the plasma is delayed backwards with the increase of plasma density

increases, the interaction range between the electron beam and the plasma increases, and the radiation bandwidth and frequency also increase accordingly, as shown in Figures 5 and 8.

Conclusion

This article establishes a mathematical model for the interaction between electron beams and plasma and derives the dispersion relationship of electron beam plasma radiation in a transverse magnetic field. During the process of high-energy electron beams passing through plasma, they are affected by a transverse magnetic field, which changes the direction of electron beam motion and causes electrons to move around magnetic field lines. Therefore, the generated radiation frequency and z-direction wave vector k are not only affected by the electron beam and plasma density but also by the transverse magnetic field. As the magnetic field increases, the radiation frequency increases but the radiation bandwidth correspondingly decreases. Increasing the electron beam velocity, electron density, or plasma density can increase the radiation frequency and bandwidth.

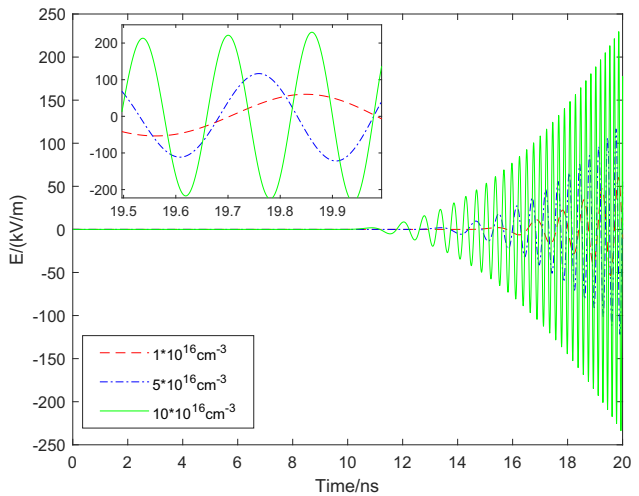

Figure 10. The variation curve of electric field over time (Different electron beam electron densities)

Simulation analysis of electric field strength under different electron beam electron densities.

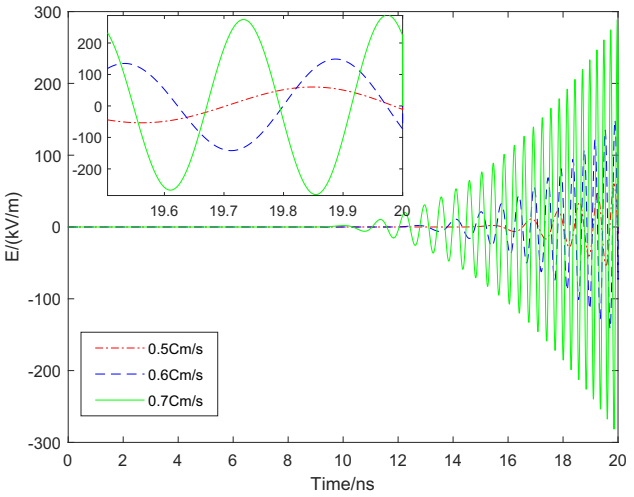

Figure 11. The variation curve of electric field over time (Different electron beam electron velocities)

Simulation analysis of electric field strength under different electron beam electron velocities. As increase in the electron beam current (increasing the electron density or speed of the electron beam) not only increases the radiation frequency of the electric field, but also increases the radiation intensity of the electric field.

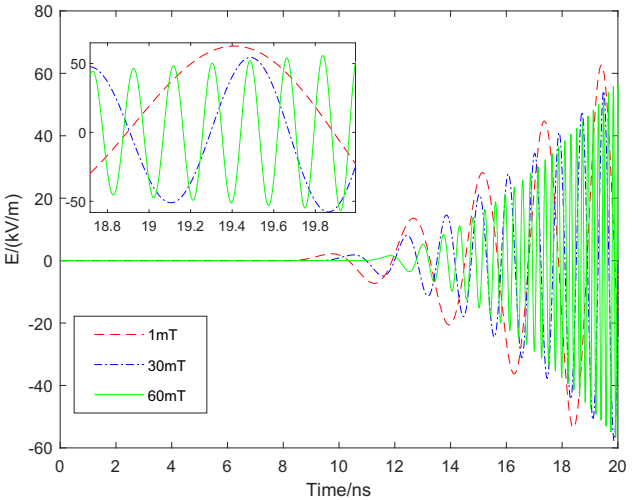

Figure 12. The variation curve of electric field over time (Different transverse magnetic fields)

Simulation analysis of electric field strength under different transverse magnetic fields. As the magnetic field increases, the radiation frequency also increases.

RESOURCE AVAILABILITY

Lead contact

Further information and requests for resources should be directed to and will be fulfilled by the lead contact, Shen Gao (gs59519829@126.com).

Materials availability

This study did not generate new unique reagents.

Data and code availability

- All data reported in this paper will be shared by the lead contact upon request.
- Partial original code (Code for figures in field matching and perturbation methods) is available in this paper's supplemental information. The simulation code involves the frequency characteristics of large signals, and due to the confidentiality requirements of special projects, it is currently not allowed to be disclosed
- Any additional information required to reanalyze the data reported in this paper is available from the lead contact upon request.

ACKNOWLEDGMENTS

This research received no external funding

AUTHOR CONTRIBUTIONS

Theoretical derivation and result analysis, S.G.; writing papers, J.X.L; plotting, J.K.Z.

DECLARATION OF INTERESTS

The authors declare no competing interests.

STAR★METHODS

Detailed methods are provided in the online version of this paper and include the following:

- KEY RESOURCES TABLE
- EXPERIMENTAL MODEL AND STUDY PARTICIPANT DETAILS
- METHOD DETAILS

Appendix

$$m_e n_{p0}\frac{\partial u_{p1}}{\partial t} + e n_{p0}\left(E_1 + \vec{u}_{p1}\times\vec{B}_0\right) = 0 \quad \text{(Equation 88)}$$

$$\gamma_0 m_e\left\{\frac{\partial}{\partial t} + u_b\cdot\nabla\right\}u_b + \frac{u_b}{C^2}eE\cdot u_b = -e(E + u_b\times B) \quad \text{(Equation 89)}$$

$$\nabla\times\vec{E}_1 = -\frac{\partial\vec{B}_1}{\partial t} \quad \text{(Equation 90)}$$

$$\nabla\times\vec{B}_1 = \mu_0 J_1 + \frac{1}{C^2}\frac{\partial\vec{E}_1}{\partial t} \quad \text{(Equation 100)}$$

$$J_1 = -en_{p0}u_{p1} - en_{b0}u_{b1} \quad \text{(Equation 101)}$$

Equation 90 Left

$$\nabla\times\vec{E}_1 = \left(\frac{\partial E_{1z}}{\partial y} - \frac{\partial E_{1y}}{\partial z}\right)\vec{x} + \left(\frac{\partial E_{1y}}{\partial z} - \frac{\partial E_{1z}}{\partial x}\right)\vec{y} + 0 \quad \text{(Equation 102)}$$

Using

$$\frac{\partial E_{1z}}{\partial y} = ik_y E_1 \text{ and } \frac{\partial E_{1y}}{\partial z} = ik_z E_{1y} \text{ so}$$

$$\nabla\times\vec{E}_1 = (ik_y E_{1z} - ik_z E_{1y})e^{i\left(\vec{k}_y\cdot\vec{y} + \vec{k}_z\cdot\vec{z} - \omega t\right)} \quad \text{(Equation 103)}$$

Equation 90 Right

$$\frac{\partial\vec{B}_1}{\partial t} = -i\omega B_1 e^{i\left(\vec{k}_y\cdot\vec{y} + \vec{k}_z\cdot\vec{z} - \omega t\right)} \quad \text{(Equation 104)}$$

So

$$k_y E_{1z} - k_z E_{1y} = \omega B_1 \quad \text{(Equation 105)}$$

Using

$$u_p = ue^{i\left(\vec{k}_y\cdot\vec{y} + \vec{k}_z\cdot\vec{z} - \omega t\right)} = \left(u_{py}\vec{y} + u_{pz}\vec{z}\right)e^{i\left(\vec{k}_y\cdot\vec{y} + \vec{k}_z\cdot\vec{z} - \omega t\right)} \quad \text{(Equation 106)}$$

Equation 88, we obtain

$$-i\omega m_e n_{p0}u_p + en_{p0}\left(E_{1y}\vec{y} + E_{1z}\vec{z}\right)e^{i\left(\vec{k}_y\cdot\vec{y} + \vec{k}_z\cdot\vec{z} - \omega t\right)} + en_{p0}\vec{u}_p\times\vec{B}_0 = 0 \quad \text{(Equation 107)}$$

Solving Equation 107

$$-i\omega m_e u_{py} + eE_{1y} + eu_{pz}B_0 = 0 \quad \text{(Equation 108)}$$

$$-i\omega m_e u_{pz} + eE_{1z} - eu_{py}B_0 = 0 \quad \text{(Equation 109)}$$

Using Equation 89 , we obtain

$$\gamma_0 m_e\left\{-i\omega + u_{b0z}\frac{\partial}{\partial z}\right\}\left(u_{bz} + u_{by}\right) + \frac{u_{b0z}^2}{C^2}eE_z + e\left(E_y + E_z - u_{by}B_0 + u_{bz}B_0\right) = 0 \quad \text{(Equation 110)}$$

Solving Equation 110

$$\gamma_0 m_e(-i\omega + ik_z u_{b0z})u_{bz} + \left(\frac{u_{b0z}^2}{C^2} + 1\right)eE_z - eu_{by}B_0 = 0 \quad \text{(Equation 111)}$$

$$\gamma_0 m_e(-i\omega + ik_z u_{b0z})u_{by} + eE_y + eu_{bz}B_0 = 0 \quad \text{(Equation 112)}$$

Equation 100, Left

$$\nabla\times\vec{B}_1 = \frac{\partial B_{1x}}{\partial z}\vec{y} - \frac{\partial B_{1x}}{\partial y}\vec{z} = ik_z B_{1x}\vec{y} - ik_y B_{1x}\vec{z} \quad \text{(Equation 113)}$$

Equation 100, Right

$$-en_{p0}\mu_0\left(u_{py}\vec{y} + u_{pz}\vec{z}\right) - en_{b0}\mu_0\left(u_{by}\vec{y} + u_{bz}\vec{z}\right) - \frac{i\omega}{C^2}\left(E_{1y}\vec{y} + E_{1z}\vec{z}\right) \quad \text{(Equation 114)}$$

We obtain

$$ik_z B_{1x} = -en_{p0}\mu_0 u_{py} - en_{b0}\mu_0 u_{by} - \frac{i\omega}{C^2}E_{1y} \quad \text{(Equation 115)}$$

$$ik_y B_{1x} = en_{p0}\mu_0 u_{pz} + en_{b0}\mu_0 u_{bz} + \frac{i\omega}{C^2}E_{1z} \quad \text{(Equation 116)}$$

Using Equations 108 and 109

$$\begin{cases} u_{py} = -i\dfrac{1}{\left[1-\left(\frac{\omega_{ce}}{\omega}\right)^2\right]}\dfrac{\omega_{ce}}{\omega}\dfrac{E_{1y}}{B_0} - \dfrac{1}{\left[1-\left(\frac{\omega_{ce}}{\omega}\right)^2\right]}\left(\dfrac{\omega_{ce}}{\omega}\right)^2\dfrac{E_{1z}}{B_0} \\ u_{pz} = -i\dfrac{1}{\left[1-\left(\frac{\omega_{ce}}{\omega}\right)^2\right]}\dfrac{\omega_{ce}}{\omega}\dfrac{E_{1z}}{B_0} + \dfrac{1}{\left[1-\left(\frac{\omega_{ce}}{\omega}\right)^2\right]}\left(\dfrac{\omega_{ce}}{\omega}\right)^2\dfrac{E_{1y}}{B_0} \end{cases} \quad \text{(Equation 117)}$$

Where

$$\omega_{ce} = \frac{eB_0}{m_e} \quad \text{(Equation 118)}$$

Using Equations 111 and 112

$$\begin{cases} u_{by} = \dfrac{\frac{i\omega_{ce}}{\gamma_0(k_z u_{b0z}-\omega)}}{\left[1-\left(\frac{\omega_{ce}}{\gamma_0(k_z u_{b0z}-\omega)}\right)^2\right]}\dfrac{E_y}{B_0} - \dfrac{\left(\frac{\omega_{ce}}{\gamma_0(k_z u_{b0z}-\omega)}\right)^2\left(\frac{u_{b0z}^2}{C^2}+1\right)}{\left[1-\left(\frac{\omega_{ce}}{\gamma_0(k_z u_{b0z}-\omega)}\right)^2\right]}\dfrac{E_z}{B_0} \\ u_{bz} = \dfrac{\frac{i\omega_{ce}}{\gamma_0(k_z u_{b0z}-\omega)}\left(\frac{u_{b0z}^2}{C^2}+1\right)}{\left[1-\left(\frac{\omega_{ce}}{\gamma_0(k_z u_{b0z}-\omega)}\right)^2\right]}\dfrac{E_z}{B_0} + \dfrac{\left(\frac{\omega_{ce}}{\gamma_0(k_z u_{b0z}-\omega)}\right)^2}{\left[1-\left(\frac{\omega_{ce}}{\gamma_0(k_z u_{b0z}-\omega)}\right)^2\right]}\dfrac{E_y}{B_0} \end{cases} \quad \text{(Equation 119)}$$

Introducing Equation 105 into Equations 115 and 116

$$ik_z\left(\frac{k_y}{\omega}E_{1z} - \frac{k_z}{\omega}E_{1y}\right) = -en_{p0}\mu_0 u_{py} - en_{b0}\mu_0 u_{by} - \frac{i\omega}{C^2}E_{1y} \quad \text{(Equation 120)}$$

$$ik_y\left(\frac{k_y}{\omega}E_{1z} - \frac{k_z}{\omega}E_{1y}\right) = en_{p0}\mu_0 u_{pz} + en_{b0}\mu_0 u_{bz} + \frac{i\omega}{C^2}E_{1z} \quad \text{(Equation 121)}$$

Introducing Equations 117, 119 into Equation 120

$$\begin{aligned} ik_z\left(\frac{k_y}{\omega}E_{1z} - \frac{k_z}{\omega}E_{1y}\right) = &\left(i\frac{1}{\left[1-\left(\frac{\omega_{ce}}{\omega}\right)^2\right]}\frac{\omega_{pe}^2}{C^2}\frac{E_{1y}}{\omega}\right. \\ &\left. + \frac{\omega_{pe}^2}{C^2}\frac{1}{\left[1-\left(\frac{\omega_{ce}}{\omega}\right)^2\right]}\left(\frac{\omega_{ce}}{\omega}\right)^2\frac{E_{1z}}{\omega_{ce}}\right) - \frac{i\omega}{C^2}E_{1y} \\ &+ \left(-\frac{i}{\frac{\gamma_0(k_z u_{b0z}-\omega)}{\left[1-\left(\frac{\omega_{ce}}{\gamma_0(k_z u_{b0z}-\omega)}\right)^2\right]}}\frac{\omega_{be}^2}{C^2}E_y\right. \\ &\left. + \frac{\left(\frac{\omega_{ce}}{\gamma_0(k_z u_{b0z}-\omega)}\right)^2\left(\frac{u_{b0z}^2}{C^2}+1\right)}{\left[1-\left(\frac{\omega_{ce}}{\gamma_0(k_z u_{b0z}-\omega)}\right)^2\right]}\frac{\omega_{be}^2}{C^2}\frac{E_z}{\omega_{ce}}\right) \end{aligned} \quad \text{(Equation 122)}$$

Where

$$\omega_{be}^2 = \frac{e^2 n_{b0}}{m_e\varepsilon_0}, \omega_{pe}^2 = \frac{e^2 n_{p0}}{m_e\varepsilon_0}, C^2 = \frac{1}{\mu_0\varepsilon_0} \quad \text{(Equation 123)}$$

Introducing Equation 117, 119 into Equation 121

$$\begin{aligned} ik_y\left(\frac{k_y}{\omega}E_{1z} - \frac{k_z}{\omega}E_{1y}\right) = &\left(-i\frac{1}{\left[1-\left(\frac{\omega_{ce}}{\omega}\right)^2\right]}\frac{\omega_{pe}^2}{C^2}\frac{E_{1z}}{\omega}\right. \\ &\left. + \frac{1}{\left[1-\left(\frac{\omega_{ce}}{\omega}\right)^2\right]}\left(\frac{\omega_{ce}}{\omega}\right)^2\frac{\omega_{pe}^2}{C^2}\frac{E_{1y}}{\omega_{ce}}\right) \\ &+ \left(\frac{\frac{i}{\gamma_0(k_z u_{b0z}-\omega)}\left(\frac{u_{b0z}^2}{C^2}+1\right)}{\left[1-\left(\frac{\omega_{ce}}{\gamma_0(k_z u_{b0z}-\omega)}\right)^2\right]}\frac{\omega_{be}^2}{C^2}E_z\right. \\ &\left. + \frac{\left(\frac{\omega_{ce}}{\gamma_0(k_z u_{b0z}-\omega)}\right)^2}{\left[1-\left(\frac{\omega_{ce}}{\gamma_0(k_z u_{b0z}-\omega)}\right)^2\right]}\frac{\omega_{be}^2}{C^2}\frac{E_y}{\omega_{ce}}\right) + \frac{i\omega}{C^2}E_{1z} \end{aligned} \quad \text{(Equation 124)}$$

Simplification Equation 122

$$\begin{aligned} &\left[i\frac{1}{\left[1-\left(\frac{\omega_{ce}}{\omega}\right)^2\right]}\frac{\omega_{pe}^2}{C^2}\frac{1}{\omega} - \frac{\frac{i}{\gamma_0(k_z u_{b0z}-\omega)}}{\left[1-\left(\frac{\omega_{ce}}{\gamma_0(k_z u_{b0z}-\omega)}\right)^2\right]}\frac{\omega_{be}^2}{C^2} - \frac{i\omega}{C^2} + ik_z\frac{k_z}{\omega}\right]E_{1y} + \\ &\left[\frac{\omega_{pe}^2}{C^2}\frac{1}{\left[1-\left(\frac{\omega_{ce}}{\omega}\right)^2\right]}\left(\frac{\omega_{ce}}{\omega}\right)^2\frac{1}{\omega_{ce}} + \frac{\left(\frac{\omega_{ce}}{\gamma_0(k_z u_{b0z}-\omega)}\right)^2\left(\frac{u_{b0z}^2}{C^2}+1\right)}{\left[1-\left(\frac{\omega_{ce}}{\gamma_0(k_z u_{b0z}-\omega)}\right)^2\right]}\frac{\omega_{be}^2}{C^2}\frac{1}{\omega_{ce}}\right. \\ &\left. - ik_z\frac{k_y}{\omega}\right]E_{1z} = 0 \end{aligned} \quad \text{(Equation 125)}$$

Simplification Equation 124

$$\begin{aligned} &\left[-i\frac{1}{\left[1-\left(\frac{\omega_{ce}}{\omega}\right)^2\right]}\frac{\omega_{pe}^2}{C^2}\frac{1}{\omega} + \frac{\frac{i}{\gamma_0(k_z u_{b0z}-\omega)}\left(\frac{u_{b0z}^2}{C^2}+1\right)}{\left[1-\left(\frac{\omega_{ce}}{\gamma_0(k_z u_{b0z}-\omega)}\right)^2\right]}\frac{\omega_{be}^2}{C^2} + \frac{i\omega}{C^2}\right. \\ &\left. - ik_y\frac{k_y}{\omega}\right]E_{1z} + \left[\frac{1}{\left[1-\left(\frac{\omega_{ce}}{\omega}\right)^2\right]}\left(\frac{\omega_{ce}}{\omega}\right)^2\frac{\omega_{pe}^2}{C^2}\frac{1}{\omega_{ce}}\right. \\ &\left. + \frac{\left(\frac{\omega_{ce}}{\gamma_0(k_z u_{b0z}-\omega)}\right)^2}{\left[1-\left(\frac{\omega_{ce}}{\gamma_0(k_z u_{b0z}-\omega)}\right)^2\right]}\frac{\omega_{be}^2}{C^2}\frac{1}{\omega_{ce}} + ik_y\frac{k_z}{\omega}\right]E_{1y} = 0 \end{aligned} \quad \text{(Equation 126)}$$

Using

$$k_y = k_z = k$$

If Equations 125 and 126 have solutions, then the coefficient determinant is 0. We obtain

$$\begin{aligned}
&\frac{1}{\left[1-\left(\frac{\omega_{ce}}{\omega}\right)^2\right]^2}\left(\frac{\omega_{pe}^2}{C^2}\right)^2\left[\frac{1}{\omega^2}-\left(\frac{\omega_{ce}}{\omega}\right)^4\frac{1}{\omega_{ce}^2}\right]\\
&-\frac{1}{\left[1-\left(\frac{\omega_{ce}}{\omega}\right)^2\right]}\frac{\omega_{pe}^2\omega_{be}^2}{\omega C^4}\frac{\frac{1}{\gamma_0(k_z u_{b0z}-\omega)}}{\left[1-\left(\frac{\omega_{ce}}{\gamma_0(k_z u_{b0z}-\omega)}\right)^2\right]}\left(\frac{u_{b0z}^2}{C^2}+2\right)\\
&-2\frac{1}{\left[1-\left(\frac{\omega_{ce}}{\omega}\right)^2\right]}\frac{\omega_{pe}^2}{C^4}+2\frac{1}{\left[1-\left(\frac{\omega_{ce}}{\omega}\right)^2\right]}\frac{\omega_{pe}^2}{C^2}\frac{k_z^2}{\omega^2}+\frac{\omega^2}{C^4}-2\frac{k_z^2}{C^2}\\
&-\frac{k_z^2}{\omega}\frac{\frac{1}{\gamma_0(k_z u_{b0z}-\omega)}}{\left[1-\left(\frac{\omega_{ce}}{\gamma_0(k_z u_{b0z}-\omega)}\right)^2\right]}\frac{\omega_{be}^2}{C^2}\left(\frac{u_{b0z}^2}{C^2}+2\right)+\left(\frac{u_{b0z}^2}{C^2}\right.\\
&\left.+1\right)\frac{\left(\frac{1}{\gamma_0(k_z u_{b0z}-\omega)}\right)^2}{\left[1-\left(\frac{\omega_{ce}}{\gamma_0(k_z u_{b0z}-\omega)}\right)^2\right]^2}\frac{\omega_{be}^4}{C^4}\\
&+\frac{\frac{1}{\gamma_0(k_z u_{b0z}-\omega)}}{\left[1-\left(\frac{\omega_{ce}}{\gamma_0(k_z u_{b0z}-\omega)}\right)^2\right]}\frac{\omega}{C^2}\frac{\omega_{be}^2 u_{b0z}^2}{C^4}\\
&-\frac{1}{\left[1-\left(\frac{\omega_{ce}}{\omega}\right)^2\right]}\frac{\left(\frac{\omega_{ce}}{\gamma_0(k_z u_{b0z}-\omega)}\right)^2}{\left[1-\left(\frac{\omega_{ce}}{\gamma_0(k_z u_{b0z}-\omega)}\right)^2\right]}\frac{\omega_{pe}^2\omega_{be}^2}{C^4}\left(\frac{1}{\omega}\right)^2\left[1\right.\\
&\left.+\left(\frac{u_{b0z}^2}{C^2}+1\right)\right]-\frac{\left(\frac{\omega_{ce}}{\gamma_0(k_z u_{b0z}-\omega)}\right)^4\left(\frac{u_{b0z}^2}{C^2}+1\right)}{\left[1-\left(\frac{\omega_{ce}}{\gamma_0(k_z u_{b0z}-\omega)}\right)^2\right]^2}\frac{\omega_{be}^4}{C^4}\frac{1}{\omega_{ce}^2}\\
&-i\frac{k_z^2}{\omega}\frac{\left(\frac{\omega_{ce}}{\gamma_0(k_z u_{b0z}-\omega)}\right)^2}{\left[1-\left(\frac{\omega_{ce}}{\gamma_0(k_z u_{b0z}-\omega)}\right)^2\right]}\frac{\omega_{be}^2}{C^2}\frac{1}{\omega_{ce}}\left[\frac{u_{b0z}^2}{C^2}\right]=0
\end{aligned}$$

(Equation 127)

Simplify Equation 127 and only consider the low-speed situation ($u \ll C$), we obtaining

$$n^2 = \frac{\left(\omega_{pe}^4+\omega_{be}^4\right)\left[1-\frac{\omega_{ce}^2}{\omega^2}\right]-2\left(\omega^2-\omega_{ce}^2\right)\omega_{pe}^2+\left[\omega^2-\omega_{ce}^2\right]^2-\frac{2\omega_{pe}^2\omega_{be}^2\omega_{ce}^2}{\omega^2}+2\omega_{pe}^2\omega_{be}^2}{2\left(\omega^2-\omega_{ce}^2\right)\left[\omega^2-\left(\omega_{ce}^2+\omega_{pe}^2+\omega_{be}^2\right)\right]} \quad \text{(Equation 128)}$$

Received: April 1, 2024
Revised: July 23, 2024
Accepted: September 23, 2024
Published: September 25, 2024

REFERENCES

1. Khorashadizadeh, S.M., Mirzaye, T., and Niknam, A.R. (2015). Weakly relativistic and space charge effects in interaction of high-power microwave with plasma. Wave Random Complex *25*, 131–140.
2. Tsiklauri, D. (2010). Vlasov - maxwell, self-consistent electromagnetic wave emission simulations in the solar corona. Sol. Phys. *267*, 393–410.
3. Schmidt-Bleker, A. (2011). Nonlinear plasma waves and wave-breaking in quantum plasmas. IOP Science. *95*, 55003.
4. Reddy, C.S., Sharma, A., and Mittal, K.C. (2015). Experimental Investigations Into Pulse-Charged Spark Gap Recovery Times and Influencing Factors. IEEE Trans. Plasma Sci. *44*, 1–7.
5. Zengchao, J.I., CHEN, S., and GAO, S. (2016). Mechanism analysis of radiation generated by the beam-plasma interaction in a vacuum diode. Plasma Sci. Technol. *19*, 015003-9.
6. Tian, W., Chen, S.X., Xiao, J.x., Gai, F., and Chen, K. (2014). Judgment Criterion of Cherenkov Radiation by an Accelerated Electron Bunch in Poloidal Magnetized Plasma. Appl. Math. Inf. Sci. *8*, 1419–1423.
7. Su, D., and Tang, C.J. (2011). The interaction of electromagnetic wave and plasma wave in an electron beam-ion channel system. Phys. Plasmas *18*, 023104. https://doi.org/10.1063/1.3551699.
8. Gao, S., Chen, S.X., Chen, K., Ji, Z.C., and Chen, J. (2017). A long pulse width and high extraction rate arc plasma electron beam source. Instrum. Exp. Tech. *60*, 705–709.
9. Chen, J., Chen, S., Xiao, J., Gao, S., Cai, H., Ji, Z., and Ji, Z. (2019). Adjustable pulse width and high repetition frequency electron beam extraction from vacuum arc plasma. AIP Adv. *9*, 015122. https://doi.org/10.1063/1.5032272.
10. Zeng-Chao, J., Shi-Xiu, C., Shen, G., Chen, J., and Tian, W. (2016). Analysis on mechanism of radiating microwave from vacuum diode. Acta Phys. Sin. *65*, 145202.
11. Xiong, J., Chen, S., Tian, W., and Chen, K. (2014). The influence of the Beam Self-fields on the dispersion characteristic of EM waves in the dielectric waveguide filled with plasma. Plasma Sci. Technol. *16*, 1–5.
12. Su, D., and Tang, C.J. (2009). Electromagnetic instability in an electron beam-ion channel system. Phys. Plasmas *16*, 053101–053101-5. https://doi.org/10.1063/1.3130262.

STAR★METHODS

KEY RESOURCES TABLE

REAGENT or RESOURCE	SOURCE	IDENTIFIER
Software and algorithms		
MATLAB R2020b：Draw a graph of the derivation results using MATLAB software	The MathWorks	*RRID:SCR_001622*

EXPERIMENTAL MODEL AND STUDY PARTICIPANT DETAILS

The research in this article is focused on the theoretical and physical aspects of plasma, without any experimental content.

METHOD DETAILS

This article uses a total of three methods to derive the dispersion relationship, and the derivation process has been detailed in the article. Interested readers can derive it based on the calculation process in the article. The perturbation method considers the dispersion relationship between an electron beam and a plasma under infinite conditions; The field matching method considers the boundary conditions of various fields between the electron beam and plasma. Both of these methods assume that the physical quantity is composed of an invariant constant and a small variable. Each small variable is transformed using Fourier transform, while ignoring high-order small variables, and transformed into a linear equation system of wave-number and frequency. By solving the above algebraic equation, the expression of wave-number and frequency is obtained. Simulation analysis is obtained through the most basic numerical calculations. During the solving process, it is only to verify the correctness of the theoretical derivation above, fix the position of electromagnetic wave radiation, and solve the relationship between the variables of the equation system and time.